Food Eng Rev (2010) 2:168–203
DOI 10.1007/s12393-010-9020-6

A Review of Methods, Data and Applications of State Diagrams of Food Systems

Shyam S. Sablani · Roopesh M. Syamaladevi · Barry G. Swanson

Received: 8 September 2009 / Accepted: 30 March 2010 / Published online: 21 April 2010

Abstract Understanding of the amorphous glassy state of food systems is often crucial in determining physico-chemical characteristics and predicting stability of dehydrated and frozen foods. At the glass transition temperature (T_g) of food components, transformation from the amorphous glassy state to the liquid-like rubbery state occurs. T_g and ice-melting temperatures (T_m) of food systems are used to construct their state diagrams, in which the different physical states/phases and state/phase transitions of food components are presented in relation to temperature and concentration. A state diagram may be used to identify the appropriate processing and storage conditions of food systems. An overview of determination methods is carried out for glass transition temperature, ice-melting temperature and conditions of maximum-freeze-concentration (glass transition temperature of maximum-freeze-concentrated solution, T_g' and onset of ice-melting temperature, T_m') for food systems. The data as T_g, T_m, T_g' and T_m' are necessary for construction of state diagrams of foods. The advantages and limitations of the determination methods are discussed. Combined data for glass transition temperature, ice-melting temperature and conditions of maximum-freeze concentration for selected food systems are presented in this study. The effect of food composition on glass line, freezing/melting curve and maximum-freeze-concentration conditions is evaluated. The significance of the state diagrams in predicting the physical, chemical and microbial stability in foods is briefly examined. Glass transition concept and state diagrams are useful for describing the physical and structural stability of food systems at specific conditions, yet they are not considered as the only determining factors of chemical, biochemical and microbial stability of food systems.

Keywords Food stability · Glass transition temperature · Ice-melting temperature · Maximum-freeze-concentration · Relaxation behavior · Spectroscopic methods · Unfrozen water · Water activity

S. S. Sablani (✉) · R. M. Syamaladevi
Department of Biological Systems Engineering, Washington State University, P.O Box 646120, Pullman, WA 99164-6120, USA
e-mail: ssablani@wsu.edu

B. G. Swanson
School of Food Science, Washington State University, P.O Box 6463760, Pullman, WA 99164-6376, USA

Introduction

The amorphous state of materials is a solid state, characterized by a short-range molecular order, whereas a crystalline state has a long-range molecular order. Many food-processing techniques result in the partial or full development of an amorphous structure, caused by super-cooling of melt, mechanical creation such as milling, dehydration or vapor condensation [79]. The most common food-processing techniques that alter physical and molecular structures in foods include drying such as spray-drying, hot air-drying and freeze-drying; grinding, extrusion and rapid freezing. Components of many processed foods such as milk powder, instant coffee, infant formula, biscuits and cookies, extruded cereals, pasta, beverage mixes and culinary food powders exist in an amorphous state.

Over the years, rigorous scientific investigations have advanced our understanding of the amorphous nature of food biopolymers and state transitions (e.g., glass transitions). Glasses are often formed by progressive moisture removal or when a liquid or a rubbery system is cooled

rapidly with little or no time for the molecules to rearrange and pack into crystalline domains [82]. Glassy amorphous solids have a high viscosity range (10^{12}–10^{14} Pas), brittleness, high strength, short-range order and little molecular mobility [141]. In the amorphous glassy state, long-range cooperative motions are restricted, but vibrations and reorientation of small groups of atoms continue to occur [115]. The temperature range where a reversible transformation from a brittle glassy state to a rubbery state occurs in an amorphous component is identified as glass transition temperature (T_g). In the glass transition region, there is no discontinuity among primary thermodynamic properties such as volume, enthalpy and free energy. However, the first derivatives of these thermodynamic properties undergo marked changes in the course of a small temperature range. Discontinuity in the coefficient of thermal expansion and specific heat at the crystallization temperature is often not detected during vitrification [99]. The glassy to rubbery state transition occurs over a temperature range without a first-order phase change, while it exhibits the characteristics of a second-order thermodynamic transition. The molecular mobility of a food system decreases as food solids transform from a rubbery state to a glassy state during cooling and/or removal of a plasticizer. The physical state and state/phase transitions of amorphous components of food biopolymers are integral to the characterization of molecular stability during processing and storage. State diagrams are used to map the physical states during state/phase transitions in amorphous food components as a function of temperature and solid or water content. Scientific understanding of glass transition phenomena in materials has progressed significantly in the last 80 years. White and Cakebread [218] first highlighted how glassy behavior in foods affects stability. Since then, many studies have explored the application of the glass transition concept to the description of food properties and various kinetic phenomena, including Slade and Levine [199, 200], Karel et al. [94], Roos [162–164], Roos and Karel [157, 158], Blanshard [23], Kalichevsky et al. [90], Kokini et al. [104, 105] and Simatos et al. [194, 195]. Glass transition involves rapid changes in the physical, mechanical, electrical and thermal properties of foods. Calorimetric studies for the characterization of state transitions dominate the food literature [142, 162]. Mechanical methods including dynamic mechanical thermal analysis, thermo-mechanical analysis and rheological techniques for the study of glass transition in food are increasingly more sensitive, but their applications to use with foods are limited. Kalichevsky et al. [90] and Kasapis et al. [96] investigated the use of mechanical spectroscopy for the study of glass transition in food biopolymers. Their studies used dynamic mechanical loss determinations and dielectric loss determinations to probe the time scales of molecular motion in the region of glass transition. These relaxation studies apply a sinusoidal external field and response of the material to the external field. In a mechanical experiment, the response is an oscillating stress or strain, while in dielectric studies, an oscillating electric field is determined as a function of the frequency of the applied field. The use of advanced spectroscopic methods, such as nuclear magnetic resonance (NMR) and electron spin resonance (EPR), have also been explored [2, 32, 90, 91, 156, 174]. The relaxation methods are introduced in which the decay in response to an applied pulse instead of a continuous sinusoidal wave is monitored. Data is then converted to a continuous wave format with Fourier transforms. This technique is used to determine ^{1}H and ^{13}C nuclear magnetic relaxation. Pulse sequences allow determination of the spin–lattice relaxation time of the system at the nuclear magnetic resonance frequency. Since this technique observes the rate of dissipation of nuclear spin energy into the molecular lattice, results are comparable with high-frequency dielectric or mechanical determinations [7].

In low and intermediate-moisture food systems, water activity (a_w) is traditionally used as a predictive tool for microbial, chemical and physical changes [124, 145]. However, the state of water and solids in foods, kinetic changes and the physicochemical stability of intermediate-moisture food polymers in a non-equilibrium state may be better explained with the glass transition concept [69, 162, 163, 200]. Studies of the relationship between glass transition, water content and food properties are advancing our understanding of physical changes [5, 18, 90, 93, 138, 157, 191] and as well as chemical changes in foods [13, 30, 55, 95, 133, 179, 184, 190].

Freezing increases the stability of foods at subzero temperatures by reducing the availability of the water for chemical, microbial and enzymatic reactions [73]. The amount of ice crystallized at temperatures below the initial freezing point depends on the temperature of the food system, the concentration of food solids and the time and temperature history of the food. However, with decreasing temperatures under adequate cooling rates, maximum-freeze-concentration is reached, in which maximum ice crystallization occurs simultaneously with unfrozen water in the food matrix [118, 119]. Maximum-freeze-concentration is characterized by high viscosity. Glass formation may start inside the food matrix at temperatures below T_m' (onset of ice melting). Type of food constituents and freezing temperature may also play a role in the nature and amount of ice crystallization [24, 72, 194, 219]. The glass transition temperature corresponding to maximum-freeze-concentration is noted as T_g', and the resulting water content from the state diagram is the unfrozen water in the matrix (X_w'). This water is freezable and not bound, but remains unfrozen during the practical time frame of observation due to its increased

viscosity [68]. Ice crystal growth is restricted due to the reduced translational and rotational motions of molecules. High viscosity rather than any binding force such as the presence of strong chemical bonds (hydrogen bonds) keeps the water from freezing [68]. Larger amounts of unfrozen water are present in foods with smaller effective molecular weight, such as fruits and vegetables. Unfrozen water may influence the physicochemical deteriorative reactions in foods since liquid water is less organized and more unstable than ice [219]. Below T_g', the viscosity becomes great enough to reduce rates of chemical reactions [21, 164]. An increase in temperature above the T_m' may result in ice melting, an increase in the amount of unfrozen water, and reduced viscosity. This reduced viscosity results in an increase in molecular mobility and leads to enhanced rates of diffusion-controlled reactions [21, 116]. State diagrams can also be used to study the stability of frozen foods [19, 27, 73, 74, 80, 152, 167]. For example, T_g' and T_m' can be used to predict loss of quality including changes in texture, aroma, caking and stickiness of freeze-dried foods [157, 166]. A few excellent reviews cover selected aspects of the glass transition concept and state diagrams [33, 99, 142, 162]. Our work reviews determination methods and data on glass transition temperatures, ice-melting temperature and conditions of maximum-freeze-concentration of food systems. Our work also explores the importance of state diagrams and how they affect the physical, chemical and microbial stability of foods.

State Diagrams

State diagrams are graphical representations of the physical states of food constituents with respect to the temperature, water or solids content of foods at constant pressure for equilibrium and non-equilibrium systems [164]. Figure 1 presents a typical state diagram. State diagrams of materials are similar to phase diagrams presenting physical states, temperature, pressure and volume of foods at equilibrium [164]. State diagrams are extended phase diagrams that provide information on equilibrium phases and non-equilibrium states of food systems [153]. State diagrams of food systems may be developed considering them as binary systems consisting of the water and the major solids or total solids present in food systems [153]. State diagrams can be used to observe and predict state changes during processing and storage of fresh, frozen, intermediate-moisture or low-moisture foods. A dynamic map or dynamic state diagram includes the equilibrium and non-equilibrium thermodynamics of food systems using temperature (Fig. 2), with solids content and time as axes [200]. The equilibrium regions are not time-dependent and can be represented using a phase diagram where non-equilibrium regions are

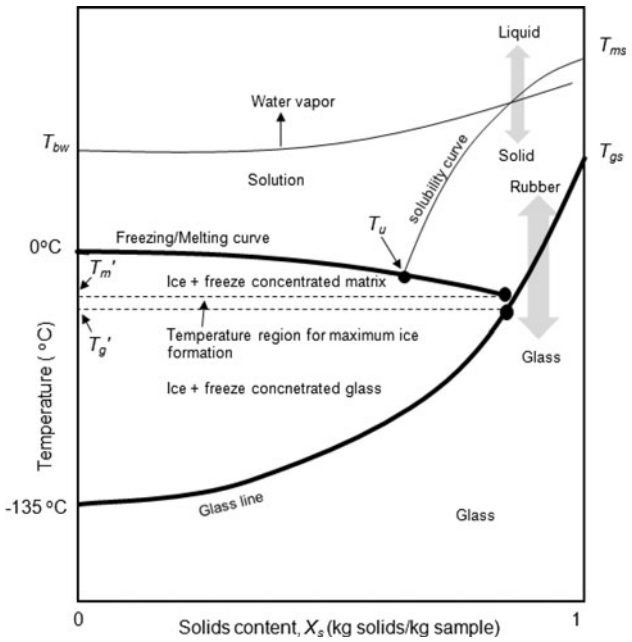

Fig. 1 A typical state diagram presenting selected regions and states of food systems. The state diagram presents glass line (dependence of T_g on water content), freezing curve (freezing point depression), solubility, T_{bw}, boiling point; T_{ms}, melting point of dry solids; T_u, eutectic point; T_m', onset ice-melting temperature in a maximally freeze-concentrated solution; T_g', glass transition temperature in a maximally freeze-concentrated solution; T_{gs}, glass transition temperature of dry solids

kinetically dependent and represented using t/τ as the third axis, where τ is the relaxation time. The dynamic map of food systems focuses on two aspects such as water dynamics and glass dynamics. Water dynamics deal with the reactivity and mobility of water as a diluent in the rubbery state of a food system. Non-equilibrium amorphous food systems approach equilibrium over extended time periods when they are stored below their glass transition temperature. Glass dynamics describe the time–temperature dependence on selected properties of a glassy food system. More details on glass and water dynamics are presented elsewhere [199, 200].

State diagrams of plant- and animal-based food systems developed during the last two decades highlight the relevance of state transition in foods during processing and storage. Heat and water are the major plasticizing agents in foods and affect the physical states and functionalities of foods during processing and storage. Selection of appropriate temperatures and humidity conditions during food-processing operations and storage is important for improving the quality and shelf lives of foods. However, since foods are complex mixtures of components with heterogeneous behavior, state diagrams may only partially explain physicochemical changes in food systems. Changes in food properties during processing and storage also depend on other factors including water activity, pH,

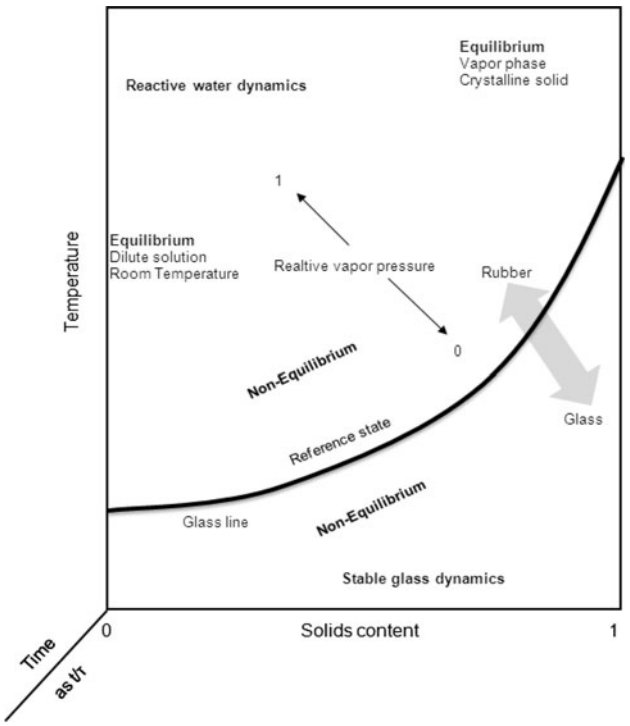

Fig. 2 A three-dimensional dynamic map or dynamic state diagram presenting equilibrium and non-equilibrium regions of food systems in relation to the temperature, solids content and time. The kinetic dependence of non-equilibrium thermodynamics of food systems may be described using a dynamic map (Adapted from [199])

presence/absence of oxygen, preservatives, antioxidants and presence/absence of catalysts [15, 115, 142, 149].

Components of a State Diagram

State diagrams present temperature–concentration relationships for both equilibrium and non-equilibrium states and represent selected physical states of foods (Fig. 1). A state diagram may include a glass line that characterizes glass transition temperature and the solids content relationship of a polymer mixture, a melting/freezing curve that designates melting/freezing point depression dependent on solids concentration, a solubility curve of solids concentration in saturated aqueous solutions at given temperatures, eutectic temperature, boiling temperature, maximum-freeze-concentration conditions corresponding to the temperature at the onset of ice melting (T_m'), and the glass transition temperature at maximum ice formation conditions (T_g') [142]. State diagrams are valuable tools in the characterization of amorphous food systems [164, 200]. A state diagram can effectively be used to analyze deteriorative reactions in foods and optimize processing conditions for maximum utility [149]. State diagrams are often based on equations such as the Gordon–Taylor and Clausius–Clapeyron equations for experimental data.

Glass Line

The influence of water or solids content on glass transition temperature at constant pressure may be presented by plotting the glass line, with temperature as the ordinate and water content or solids content as the abscissa. Unlike the equilibrium lines in a phase diagram, the glass line in a state diagram differentiates the general states of non-equilibrium systems such as a stable glassy state and the metastable rubbery state. The glass line for a food system is dependent on composition, water content, molecular weight of the biopolymers and degree of polymerization [208]. The T_g of food solids increases as biopolymer molecular weights, size, rigidity and cross-linkages increase and decreases as biopolymer chain flexibility increases. Incompatible constituents and heterogeneous complex food systems often lead to the detection of more than one glass transition temperature [126, 208]. A small amount of free water can drastically lower the glass transition temperature of dry food solids. The plasticizing ability of water is attributed to its low molecular weight and to its low glass transition temperature (−135 °C), compared to the glass transition temperature and hydrogen-bonding capacity of food biopolymers [208].

Glass Transition Theories

Several theories including free volume, kinetics and thermodynamics attempt explain glass transition phenomena. Recent reviews by Abiad et al. [1] and Roos [169] present a detailed discussion of relevant theories. These theories are applied to predict glass transitions of foods and pharmaceuticals with some success [1]. A brief description of three major theories of glass transition is presented in the following text.

Free Volume Theory

Free or unoccupied volume allows segmental mobility in a material, unlike occupied volume. Free volume theory considers a constant free or unoccupied volume is reached in a material at its glass transition temperature, and this free volume remains constant in the glassy state [66]. To pinpoint the glass transition temperature, the free volume theory was employed in a quantitative fashion to interpret glassy phenomena in terms of molecular processes [54]. According to free volume theory, T_g is located at the end of a glass transition region, where free volume declines to ~3% of the total volume of a material [60, 216]. At this volume, the coefficient of thermal expansion of free volume undergoes a discontinuity, reflecting a change in slope of the linear plot of the total volume as a function of

temperature. Conformational rearrangements below T_g are small in the experimental time frame and attributed to a very small free volume. The Doolittle equation empirically relates free volume to the viscosity of the system. The temperature dependence of viscosity in the glass transition region described by William–Landel–Ferry (WLF) equation may be derived with free volume theory using the Doolittle equation [70]. The WLF equation is used to describe changes in relaxation times above the glass transition temperature. The free volume concept is used extensively by material scientists to develop a mechanistic understanding of the rubber to glass transition based on the concept of macromolecular volume. However, free volume theory does not explain the heating/cooling rate dependence on glass transition temperatures or the kinetic nature of glass transition temperatures [168].

Kinetic Theory

Kinetic theory assumes that glass transition is a dynamic process. Kinetic theory describes the molecular relaxation time of a selected polymer chain and the time scale of the experiment exhibit an equivalent order of magnitude at the glass transition temperature [70]. Glass transition is influenced by the heating or cooling rate during the experiment. Glass transition is observed at a lower temperature when slow heating rates are used. Slow heating rates are associated with long experimental time scales, wherein conformational rearrangements occur [1]. Kinetic theory explains heat capacity change greater than and less than glass transition temperatures and change in T_g with heating/cooling rates [168].

Thermodynamic Theory

Thermodynamic theory assumes that glass transition as a second-order phase transition and that equilibrium properties of glass transitions are achieved at infinite experimental time frames. According to this theory, a true equilibrium thermodynamic transition is reached when the conformational entropy of the system becomes zero at a temperature 50 °C below the experimentally determined T_g [70, 71]. Thermodynamic theory explains changes in T_g dependent on plasticizer content, molecular weight and cross-link density [168].

Characterizing Glass Transition

Glass transition is a change in state associated with a considerable change in molecular mobility and relaxation time in amorphous food solids. Properties of a food system are dramatically changed as the food system transforms from a glassy state to a rubbery state. Determination of the glass transition temperature is based on observation of changes in thermal, mechanical, dielectric, and volumetric properties and molecular mobility over the glass transition temperature range. In food biopolymers, free volume, specific heat, specific volume or the thermal expansion coefficient increase, while the elastic modulus and viscosity decrease during this transition. The glass transition temperature of food systems is dependent on the method of observation and is not always well defined. Each analytical technique probes material properties at a selected distance scale to analyze glass transition. Glass transition temperature is also affected by the heating or cooling rate, the applied frequency of oscillation and the sample history. The most common techniques such as differential scanning calorimetry and mechanical spectroscopy provide an indication of a transition at a macroscopic level, while nuclear magnetic resonance and electron spin resonance provide information on the molecular mobility in selected phases and microstructural locations. Determination of glass transition temperature for food products is further complicated because of their chemical and microstructural complexity. Glass transitions often occur over a large temperature range due to a broad distribution of relaxation times and/or to unresolved transitions corresponding to different components [115]. The glass transition temperature is taken as the onset temperature of the glass transition temperature range (onset T_g) or as a temperature corresponding to a 50% change in heat capacity occurring over the transition (midpoint T_g) in a differential scanning calorimetric determination. The temperature range of glass transitions, the changes around glass transitions and material properties at temperatures greater than the glass transition temperature are all highly dependent on food composition and molecular weights of the components. Small molecular weight components (for example, water and simple sugars) provide a glass transition over a relatively narrow temperature range (10–20 °C), whereas large molecular weight food components such as proteins and starch exhibit glass transition over a broad temperature range (as large as 50 °C) [164]. Most foods are multiphasic systems and therefore do not exhibit global glass transitions. Glass transitions are properties of food components and affected by component interactions. Distinct transitions associated with selected phases are observed with multicomponent mixtures. For instance, Mousia et al. [132] observed distinct tan δ peaks in the DMTA analysis of a mixture of gelatin, amylopectin and water with selected gelatin/amylopectin ratios, indicating the presence of two phases. The degree of hydration of each food component differs depending on the thermodynamic compatibility of the component with water. Unlike homogeneous single-phase systems, multicomponent systems are heterogeneous, so that unequal water distribution depends

on food components [132]. Considering the physicochemical stability of multiphasic systems, lower glass transition temperatures may describe a critical limit.

Glass transition characterization methods may be classified as thermal (differential scanning calorimetry [DSC] and modulated differential scanning calorimetry [MDSC]), mechanical (dynamic mechanical thermal analysis [DMTA], rheological determinations and thermal mechanical analysis [TMA]), dielectric (dielectric thermal analysis [DEA]), spectroscopic (nuclear magnetic resonance [NMR], and electron spin resonance [ESR] spectroscopy) based on the properties determined [169]. DSC traces vitrification processes by providing a direct, continuous determination of a material heat capacity, while mechanical spectroscopy probes the relaxation behavior of synthetic and biopolymers over a large temperature range and frequency scale. The mechanical loss of a material results from conformational changes leading to a phase shift between stress and strain during periodic excitation and a damping of a free vibration sample. The phase shift increases as damping increases. Damping reaches its maximum when the period of molecular motion approaches the time scale of the experiment. These mechanical loss peaks are used to pinpoint different relaxation processes [220]. Spectroscopic techniques such as NMR and EPR monitor the motional properties of molecules by detecting the relaxation characteristics of the active nuclei and the spin probe dissolved in the sample. Spectroscopic techniques are also used to characterize glass transition in biopolymers. Glass transition and relaxation determination methods are reviewed extensively in recent review articles by Abiad et al. [1] and Roos [169].

Differential Scanning Calorimetry

Differential scanning calorimetry (DSC) is the most extensively used technique for thermal transition analysis of food systems because of its unique characteristics and simplicity. DSC determines the enthalpy and temperature changes between a sample and reference during the phase and state transitions. Information on transition temperatures, enthalpy of melting/freezing, specific heat and latent heat are obtained from DSC temperature scanning of food systems [141]. Gelatinization of starch, phase transitions, crystallization or melting of polysaccharides and lipids, and the quantity of unfrozen water may be determined by using a differential scanning calorimeter. Quality assurance, adulteration of food materials and freezing-induced denaturation of food proteins may also be studied with DSC [58].

Thermal transition experiments of low and high-moisture foods are conducted with a differential scanning calorimeter after calibrating the calorimeter with selected standards. An empty, sealed aluminum pan is used as a reference in each experiment. A common procedure for DSC determinations involve a thermal scan of a small quantity ($\sim$10 mg) of food over a selected temperature range, dependent upon the food composition and water content. Glass transition temperature is kinetically governed and the rate of the thermal scan of the food influences the T_g. Scan rates of 5 and 10 °C/min are commonly used for determination of glass transition temperatures. A typical DSC thermogram is presented in Fig. 3a. The glass transition temperature (T_g) is identified as the step transition in the heat flow curve of the DSC thermogram, presenting the variation in heat flow with temperature. The midpoint of step transition is generally determined for T_g; however, most recent studies reported temperatures (onset, T_{gi}; midpoint, T_{gm}; and end point, T_{ge}) of glassy to rubbery state transitions. The onset glass transition temperature may be suitable for predicting food storage stability and shelf life. High-moisture foods are annealed to identify clear and accurate glass transition temperature ranges, achieve maximum-freeze-concentration conditions and avoid exothermic crystallization peaks [143]. A nearly complete state diagram of food systems can be constructed by plotting the glass line and melting curve using DSC results. The state diagrams of most food systems published in the literature were developed using DSC. The DSC provides direct determinations of enthalpy change during phase transitions [58]. The plasticization effects of water and interactions with food components may be studied by fitting Gordon–Taylor model with the glass transition temperature–water content data [164].

The advantages of using DSC include convenient preparation, rapid analysis, applicability to low- and high-moisture foods and a broad range of temperatures [58]. Characterizing the T_g of the individual components of food systems is relatively difficult with the DSC. Glass transition temperatures of complex food systems determined with DSC may not be accurate, although the concentrations of individual components may determine the T_g of the food system. The DSC may not provide precise specific heat transitions for foods containing food components of large molecular weight, such as starches or proteins. DSC determination of T_g is most suitable for sugar-rich foods of small molecular weight [147, 164, 181]. The kinetics of thermal transitions depends on the heating rates selected for DSC analysis, because of the thermal lag associated with the heating rates [58, 195]. Foods in the DSC are more uniformly heated when slower scan rates are applied, resulting in a small temperature lag during the analysis. A higher T_g is observed when rapid heating rates are used. Finally, DSC analysis may not be sufficiently sensitive to recognize weak glass transitions [58]. Optimizing conditions for DSC determinations is necessary to provide accurate T_g results.

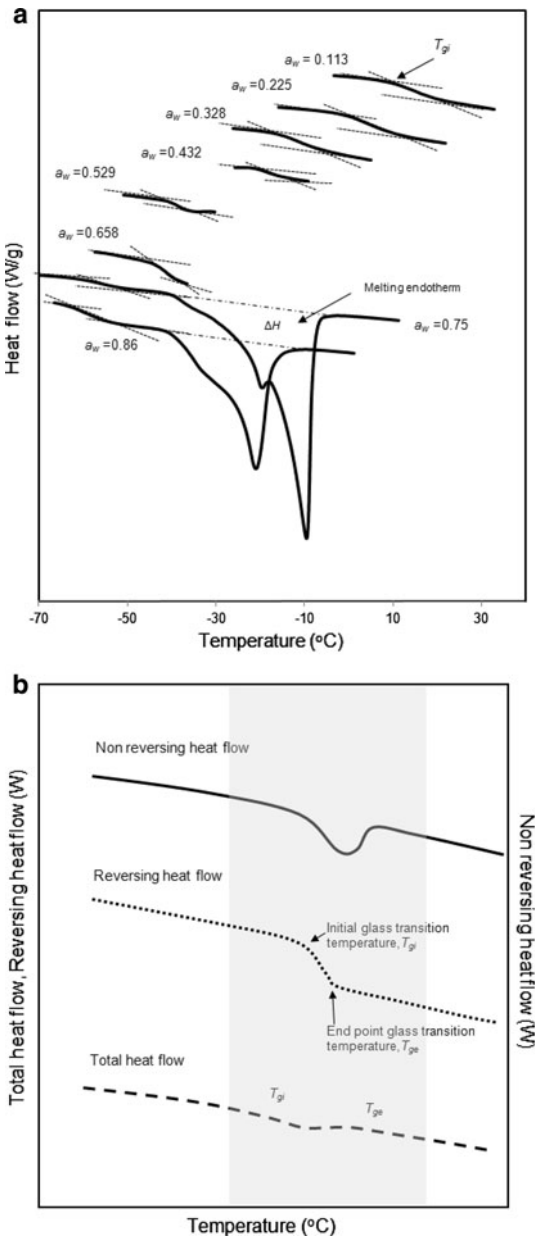

Fig. 3 **a** DSC thermogram of amorphous raspberry solids presenting heat flow versus temperature curves during desorption at selected water activities (a_{w1} = 0.113–0.86) where T_{gi} = initial glass transition temperature. Glass transition temperature decreased as water activity increased. At higher water activities, the melting endotherms were observed indicating the presence of ice where ΔH is the enthalpy of melting [202]. **b** A typical MDSC thermogram presenting total heat flow, reversing heat flow and non-reversing heat flow versus temperature T_{gi} = initial glass transition temperature, and T_{ge} = end point glass transition temperature

Modulated Differential Scanning Calorimetry

Modulated differential scanning calorimetry (MDSC) is an extension of conventional DSC and a very useful method for thermal characterization of heterogeneous food biopolymer systems. Modulated DSC is more sensitive in the detection of glass transition temperatures than conventional DSC, due to the rapid heating rate produced by sine wave modulations [112]. Sinusoidal oscillations in heating and cooling rates produce sample temperatures that change with time in a nonlinear fashion (Modulated DSC™ Compendium, [130]). The underlying principle of MDSC is that sine wave modulations deconvolute the total heat flow to reversible heat flow events related to heat capacity and non-reversible heat flow signals related to irreversible events during heating [42]. Heat capacity evaluation of foods is relatively easy and rapid with MDSC. Thermal transition experiments are conducted after calibrating the modulated differential scanning calorimeter with standard temperatures and enthalpies of fusion for indium and sapphire, as in conventional DSC. The experimental protocol involves thermal scanning of a food over a selected temperature range similar to DSC experiments. In addition, modulation temperature amplitude and modulation periods are specified. Total heat flow is made up of two components: a thermodynamic component (reversing heat flow signal in MDSC) that involves the heat capacity and rate of temperature change in a material and a kinetic component (non-reversing heat flow signal in MDSC) that involves the temperature of the material and time (Modulated DSC™ Compendium). The MDSC is useful for separating complex thermal events such as thermodynamic and kinetic relaxations. The heat capacity of the material can be calculated using heat flow amplitude, temperature amplitude and modulation period. Reversible heat flow is the product of heat capacity and average heating rate (Modulated DSC™ Compendium). The average modulated heat flow obtained with MDSC is taken as the total heat flow. The non-reversing heat flow is the difference of total and reversing heat flows (Modulated DSC™ Compendium). With the reversing heat flow, transitions with step change in the heat capacity, thermodynamic characteristics such as melting, and glass transitions are analyzed; and with non-reversing heat flow, kinetic characteristics such as molecular relaxations, crystallization and decomposition are identified (Fig. 3b) [46]. The glass transition and melting temperatures of a material are determined using the reversing heat flow curve plotted against change in temperature. Various operational parameters such as heating and cooling rates, modulation period and modulation amplitude influence the observed transitions in MDSC. Like DSC, the rate of thermal scanning may significantly affect the glass transition temperatures determined from MDSC thermograms. The amplitude of modulation temperature and modulation period may also influence the determination of glass transition temperatures. Advantages of MDSC include better detection of glass transition temperature in high-moisture foods, increased sensitivity to observe weak transitions, simplification of overlapping

complex transitions and increased resolution (Modulated DSC™ Compendium). Limited studies relate the use of MDSC for determination of glass transition temperatures in food systems, since MDSC is a relatively new technique.

Dynamic Mechanical Thermal Analysis

At temperatures near to or greater than the glass transition temperature, the solid state is transformed to a supercooled liquid state with rapid time-dependent flow. In DMTA, sinusoidal oscillatory strain or stress input is applied in foods, and the resulting stress or strain is determined [1, 34]. DMTA describes the viscoelastic characteristics of food materials by determining the storage modulus (E'), loss modulus (E'') and mechanical loss factor ($\tan\delta = E''/E'$) with the frequency of oscillating deformation as a function of temperature during state transitions of foods. E' and E'' are the ratio of in-phase and out-of-phase stress to the corresponding applied strains, respectively [34]. E' is also related to recoverable elastic energy stored in the material, while E'' is related to deformation energy dissipated as heat of friction [49]. The temperature range encompassing a sudden decrease in storage modulus (E'), a maximum of E'' or $\tan\delta$ is identified as the glass transition temperature [34]. The onset glass transition temperature is identified as the temperature where tangents from glassy and transition regions meet in the storage modulus curve, or the temperature where the maximum E'' is observed [34]. Various determination geometries with selected modes of operations such as tension, compression, shear or bending are available for the determination of viscoelastic properties of food materials [34]. In the case of parallel plate geometry, food systems are placed onto the plates and coated with a silicone grease to reduce water loss. The foods are heated in the selected temperature range at fixed strain sweeps (0.05%) and at selected frequencies ranging from 0.001 to 200 Hz with a dynamic mechanical thermal analyzer (DMTA) [90, 91, 134]. The viscoelastic properties of food powders are characterized using a powder cell in DMTA [1]. E' and E'' are components of tensile elasticity, determined when axial forces are applied. A decrease in E' and a maximum in E'' as well as $\tan\delta$ of polymers are observed at the temperature corresponding to α relaxations [33] (Fig. 4). A suitable frequency must be selected to insure that a DMTA peak coincides with the glass transition temperature [23]. At greater frequencies, higher glass transition temperatures are identified, since glass transition is a relaxation transition [34]. DMTA is more sensitive than the calorimetric method for detection of glass transition temperatures, particularly for complex food biopolymers, semicrystalline and cross-linked polymers where the change in heat capacity is small [34]. However, additional sample preparation for dynamic mechanical thermal analysis limits its applicability. For instance, food powders are melt-mixed by adding water and heated to a specific temperature and dried in molds before being subjected to analysis [64]. Samples of required dimensions are prepared for DMTA. Also, tablets are commonly prepared for DMTA by pressing at high pressures [1]. Large quantities of low-moisture solid materials are generally selected for DMTA analysis. Use of DMTA in subambient temperature ranges may be challenging, due to potential condensation [34]. Also, the temperature associated with the tan δ peak in DMTA may be higher than the glass transition temperature observed in calorimetry, due to water loss during sample preparation and heating [147]. Also, high T_g may be attributed to slow heating rates (5–10 °C) used in calorimetry, comparable to static heating [53, 147].

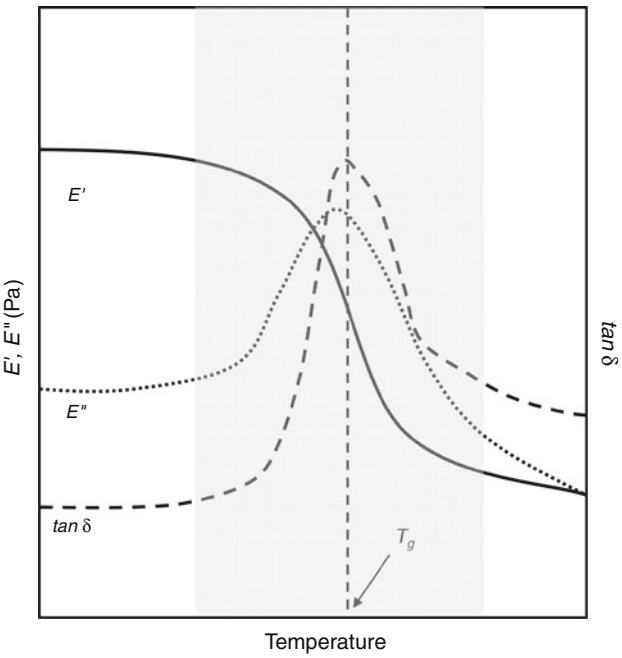

Fig. 4 A typical DMTA thermogram presenting E', E'' and tan δ versus temperature

Rheological Determinations

Rheology is used extensively by Kasapis et al. [96–99] to characterize glassy behavior of food systems. The procedure involves time–temperature superposition of mechanical spectra (shear storage modulus G' and shear loss modulus G'') obtained from rheological determinations, as well as calculating the data with the Williams–Landel–Ferry (WLF) equation based on free volume theory and the Arrhenius equation to identify glass transition temperature [97]. Rheological determinations provide the shear storage modulus (G'), which makes up the elastic component of the network, the shear loss modulus (G''), which makes up the viscous component, and the dynamic viscosity (η^*). They

are performed using a controlled strain rheometer. A small quantity (10–12 g) of food is loaded on a circular plate and coated with a silicone fluid to minimize water loss during experiments. The food is cooled below its expected T_g and scanned at 1 °C/min to a temperature higher than its T_g. The isothermal mechanical spectra are obtained at selected temperature intervals (~3 °C) between 0.1 and 100 rad/s. In these experiments, the applied strain on shear may vary from 0.0005% in the glassy state to 1% in the rubbery plateau to accommodate large changes in food stiffness. A strain sweep is performed to confirm that the small deformation analysis is carried within the linear viscoelastic region.

Figure 5a presents thermal profiles of G', G'' and tan δ for a biopolymer matrix containing 5% gelatin, 25% sucrose and 50% glucose syrup. Area I represents the glassy state with a dominant elastic component (G') greater than the viscous component (G''), with values of G' greater than 10^9 Pa. Area II represents the glass transition state and the dominant loss modulus or viscous component (G'') occurs with heat loss. Area III represents the rubbery state with value of tan δ less than one [97]. Mechanical spectra (frequency vs. G' and G'') are combined to produce a master curve of reduced frequency (frequency × shift factor) versus the superpose of shear modulus (G' and G'') [97]. A computerized calculation minimizing a multiple regression correlation coefficient is used to shift mechanical spectra and produce a master curve for viscoeleasticity. The shift factor is plotted against the temperature. The portion of the temperature dependent on the shift factor (glass transition state) is modeled using the WLF equation, while another portion (glassy state) is fitted to the Arrhenius equation (Fig. 5b). According to free volume theory, T_g is located at the end of the glass transition state, where the free volume declines to insignificant volumes (~3% of the total volume of the material). Rheological determinations may provide T_g and demarcate the onset of the glassy state from the glass transition region. In the glass transition region, transverse string-like vibrations of polymeric chains diminish with reduced temperature, whereas in the glassy state (or temperatures less than T_g), relaxation processes are heavily controlled by specific chemical features [98].

The mechanical transitions in several food systems, such as dried fish proteins and fruit carbohydrates, are difficult to determine [98, 146, 177, 178]. To circumvent the problem of a decreased glass transition temperature in dehydrated foods, another approach was suggested to assess the temperature dependence of state changes [98, 146, 177, 178]. Kasapis [98] observed that for gelatin and sugar mixtures, the T_g obtained with the time–temperature superposition principle coincides with the minimum of the storage modulus. A procedure was therefore recommended

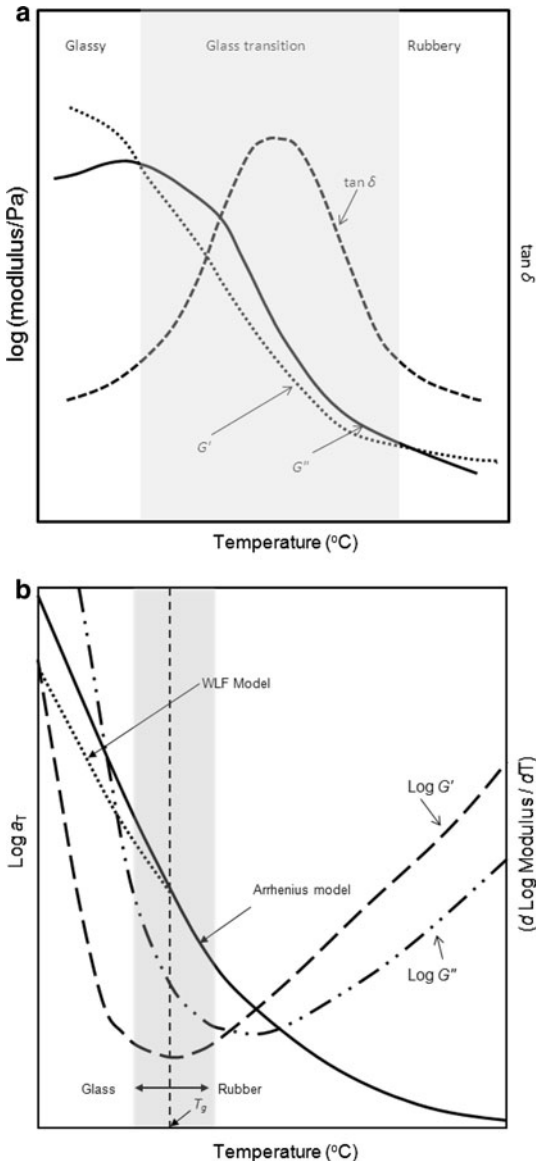

Fig. 5 **a** A schematic diagram presenting the variation of G', G'' and tan δ with temperature in a biopolymer mixture containing 5% gelatin, 25% sucrose and 50% glucose syrup. **b** A schematic diagram presenting the deviation of log a_T, first derivative of log G' and log G'' with temperature

in which a plot of the first derivative of log G' as a function of sample temperature is prepared and the minimum of the storage modulus is defined as the mechanical glass transition temperature (Fig. 5b). Mechanical transition procedures are used to determine the glass transition temperatures in dehydrated fish and fruits [98].

Thermo-Mechanical Analysis

Softening or loss of mechanical rigidity of low-moisture solids during state transitions of food systems may be

determined by a thermo-mechanical analyzer (TMA). TMA is a simple and relatively inexpensive methodology. In TMA, changes in physical dimensions (volume, length) of the foods under non-oscillatory stress are recorded as a function of temperature and time during temperature scanning [1, 56, 164]. Selected geometries and modes of operation such as compression, tension, flexure or torsion are possible with TMA [1, 56]. To observe consistent dimensions, parallel geometry of the food systems is used [72]. A dilatometer is placed in the sample holder of the thermo-mechanical analyzer, and compression or expansion mode with selected force (normally 20–50 mN for penetration mode) is maintained for 5 min at room temperature before heating. Food systems are heated over a selected temperature range at a rate of 5 °C/min, and the change in the volume/length of the sample is determined by using an expansion probe during heating [56]. Thermograms presenting the glassy and rubbery regions in the materials are analyzed, and T_g is assigned as the temperature at the intersection of the tangent lines along the glassy and rubbery regions [139]. TMA provides greater sensitivity than DSC in recognizing state transitions of amorphous and semicrystalline food components. Disadvantages of TMA include water loss during sample preparation and heating, difficulty in controlling the heating and cooling rates, and inaccuracy in assigning glass transition temperatures in porous foods [57].

A simple thermal mechanical compression test (TMCT) technique consisting of a thermally controlled sample cell attached to a texture analyzer is developed for the characterization of glass transition for food powders [25, 26]. Glass transition characterization is carried out in a thermally controlled cell using a thermal compression test in creep mode, where food is subjected to a constant compression force while it is heated, and the probe displacement is determined as a function of temperature. At the glass to rubber transition, a sudden increase in displacement is observed. The glass transition temperature is determined using the slope of linear regression line greater than the transition and a displacement value less than the transition in the displacement–temperature diagram during heating (Fig. 6). In Fig. 6, to determine T_g, the mean value of displacement is taken from points 1–2 below transition and the linear regression equation of the data points above transition (from 3 to 4). The TMCT method was tested with the standard DSC, DMTA/TMA techniques, using skim milk powder adjusted to water contents in the range of 2–5% (kg water/kg dry solids). The method was found to be accurate and sensitive for the determination of the glass transition temperatures in selected food powders [25, 26]. The TMCT method provides glass transition temperatures for foods with T_g greater than ambient temperatures. The TMCT method must be validated with a wide range of powders such as modified proteins and starches.

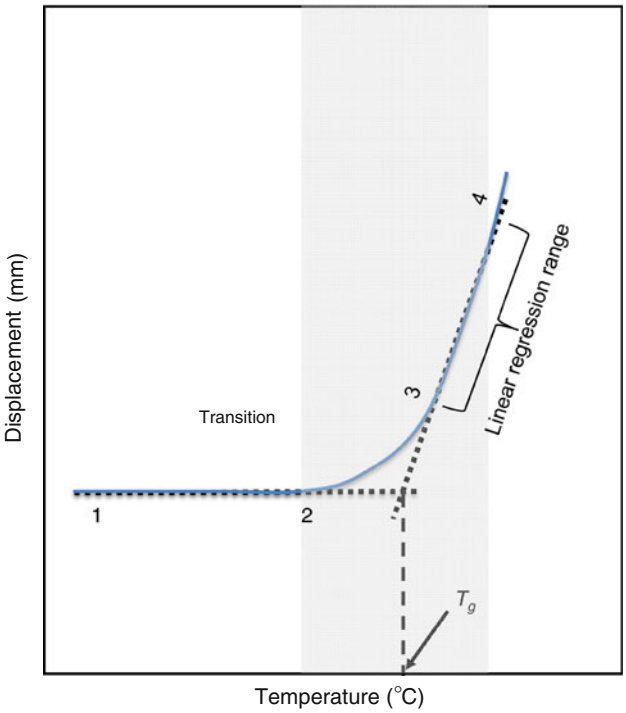

Fig. 6 A typical TMCT thermal mechanical responses during glass transitions. Glass transition temperature (T_g) is observed at the temperature where sudden change in displacement occurs. T_g is determined using the data points below transition and linear regression equation of the data points above transition (Adapted from [26])

Dielectric Thermal Analysis

The DEA/DETA method determines the relaxation behavior of a food system as it is subjected to a temperature scan over a selected polarizing frequency range [1, 110]. The dielectric cell used in DEA/DETA varies dependent on the application and material of interest [213]. Experiments are performed with a dielectric analyzer. A typical geometry of DEA is the parallel plate electrode system. Expansion and contraction of a food system during heating and cooling are the associated problems of this geometry [213].

The food system is placed between the two electrodes of a capacitor, and the impedance of the capacitor is determined during a thermal scan at selected frequencies. The food system is heated over a selected temperature range at a heating rate of approximately 1–5 °C/min for selected frequencies of 0.001 to 10^6 Hz. Dry nitrogen gas is used to avoid condensation of water on the foods. The absorption maximum corresponds to the glass transition temperatures obtained similar to the DMTA method. A suitable frequency must be selected to insure that the DEA/DETA

peak coincides with the T_g. In dielectric techniques, dielectric constant or permittivity (ε'), the degree of alignment of dipole molecules to the electric field, dielectric loss constant (ε''), the energy needed to align the dipole molecules and tan δ ($=\varepsilon''/\varepsilon'$) of food as a function of temperature/frequency for an applied stress are detected using alternating current [1, 20, 151]. Glass transition temperatures (T_g) are assigned to the temperature corresponding to an increase in the permittivity or the peak of tan δ–temperature diagram. During glass to rubber transitions, the polar groups of the food components attain mobility, resulting in increased permittivity [20]. The characteristic relaxation time (τ) associated with the increased mobility of polar groups is determined by the permittivity of the food system [20]. To make accurate determinations, the electrodes and sample food system must stay in good contact and avoid electrode polarization. Samples with large surface areas and small thicknesses are selected to improve the sensitivity of DEA/DETA. Also, electric current leakage must be minimized at the edges [20]. The DEA/DETA techniques are more sensitive than DSC and DMTA for observing phase and state transitions in a wheat dough [111]. However, DEA is not used extensively in the determination of phase and state transitions of food systems.

Nuclear Magnetic Resonance

Nuclear magnetic resonance (NMR) is a spectroscopy technique based on the magnetic properties of atomic nuclei and is used to detect molecular motion by determining the relaxation characteristics of the NMR active nuclei, such as ^{1}H, ^{2}H, ^{3}H, ^{13}C, ^{17}O, ^{23}Na and ^{31}P [106, 172]. Using ^{1}H NMR, the mobility of water was examined with respect to the T_g. A shift in the relaxation time of water that coincides with a shift in relaxation time at T_g was observed [2, 90, 91]. However, solid-state NMR studies to determine the mobility of chemical reactants and correlation of this mobility with reaction rates are lacking [189]. NMR determines the time constant T_1 (spin–lattice relaxation time), indicating longitudinal relaxation and a time constant T_2 (spin–spin relaxation time), indicating transverse relaxation. Figure 7 presents typical relaxation times (T_1 and T_2) of water as a function of temperature. When foods undergo transitions from the glassy to the rubbery state due to plasticization by water or heat, molecular mobility increases significantly and may be represented by a steep slope of the T_2–temperature relationship. However, the T_1–temperature relationship of foods is presented as a negative slope as temperature increases and reaches T_g. In general, foods exhibit an abrupt change in slope in the T_1–temperature relationship as temperature increases above T_g [172]. The relaxation

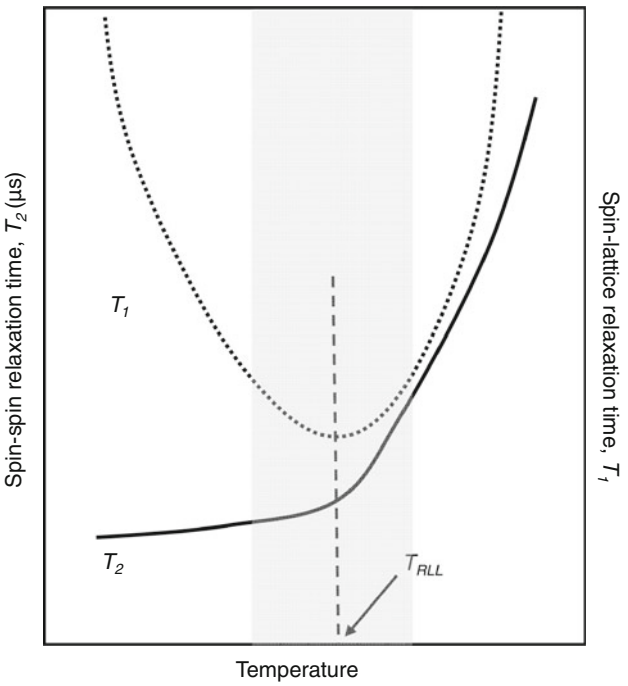

Fig. 7 A schematic diagram presenting NMR state diagram presenting spin–lattice relaxation time (T_1) and spin–spin relaxation time (T_2) of solids as a function of temperature. A sudden decrease in T_1 to certain temperature (T_{RLL}) and a sudden increase is observed. The change in T_2 is small at low temperatures, while a sudden increase in T_2 is observed after a certain temperature (T_{RLL}) (Adapted from [122])

time–temperature plot of liquids is a straight line with positive slope, while on relaxation time–temperature plots for solids, T_1 increases significantly beyond specific temperatures and T_2 exhibits a minimum value at a specific temperature corresponding to the rigid lattice limit (T_{RLL}) [23, 122]. Some studies report that NMR observed T_2 relaxation times may not always approximate glass transition temperatures [23, 89]. However, the difference between T_{RLL} and T_g may be attributed to different distance scales/levels in which different methods observe glass transition temperature. For instance, DSC presents the macroscopic mobility of a food system by determining the step change in heat capacity at the glass to rubber transition, while NMR determines the microscopic/molecular level mobility approximations in a food system. Often, the T_g values approximated from NMR are lower than the T_g values obtained using DSC [90, 186]. For instance, Kalichevsky et al. [90] reported that the midpoint T_g of amylopectin maize starch at 15% water content obtained from DSC was 56 °C, while the T_g approximated using NMR was 38 °C. The T_g observed by different methods is dependent on various factors, including principle and procedure involved in the method, sample preparation and the various experimental parameters controlling the observation [186]. The selection of a method for the

observation of T_g is often dependent on the application, the information required and the material of interest [187, 188].

Electron Spin Resonance Spectroscopy

Electron spin resonance (ESR) spectroscopy is a good method for the study of molecular motion in biological glasses and provides information on the rotational mobility of dissolved spin probes [32]. The rotational mobility of the probes is expressed in the rotational correlation time. ESR is closely related to nuclear magnetic resonance spectroscopy. When electromagnetic radiation is applied to food systems, some amount of energy is absorbed, resulting in the discharge of unpaired electrons or free radicals that are paramagnetic. The absorption of the electromagnetic radiation attributed to free unpaired electrons in the presence of an externally applied magnetic field is determined and amplified to provide an ESR spectrum [78]. A change in the ESR spectral shape represents molecular mobility during glass transitions in amorphous systems [164]. The spin probe rotational correlation time (τ_R) is determined during a thermal scan by inserting a probe of nitroxide radicals inside the food [31]. The τ_R is calculated using signal components of the ESR spectra [32]. An increase in temperature reduces τ_R and represents increased molecular mobility. An increased τ_R observed in the glassy state of foods represents decreasing molecular mobility. A sharp change in the slope of the linear relationship between log τ_R and temperature is an indicator of glassy to rubbery state transitions. A decrease in τ_R values is observed in the rubbery state (Fig. 8) because of the increase in free volume and the decrease in the viscosity of the food system [32]. The use of ESR for observation of state and phase transitions in food systems is limited. Rolee and LeMeste [156] analyzed the rotational diffusion coefficient for starch–water systems of intermediate-moisture contents at selected temperatures using ESR. One disadvantage of ESR is that the rotational relaxation time and the molecular mobility of the external probe introduced into the matrix are approximated using the component signals rather than the relaxation times of matrix itself, unlike NMR that approximates the relaxation time and molecular mobility of the food [32].

Characterizing the Effects of Water and Other Plasticizers

Water is the universal solvent, a common additive and a plasticizing agent in food systems. Adding thermal energy can also plasticize foods and decrease the T_g of the food systems by increasing the molecular energy as well as the entropy of food systems. The extent of the T_g decreasing capacity of the plasticizing agent in foods depends on the concentration of plasticizing agent, its molecular weight, glass transition temperature, viscosity and compatibility with food solids [91, 163, 173].

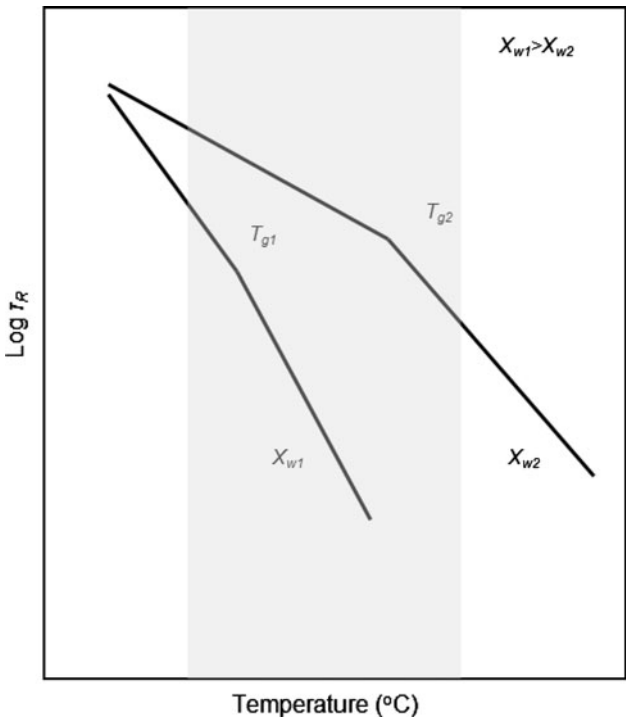

Fig. 8 A schematic diagram presenting log τ_R as a function of temperature by ESR study. Glass transitions observed (T_{g1} and T_{g2}) for different water contents (X_{w1} and X_{w2})

The plasticizing effect of water is attributed to a large dielectric constant and the ability to promote hydrogen bonding among hydrophilic molecules during plasticization [126]. In dry and intermediate-moisture food systems, the T_g of the system decreases sharply with increase in water content, while in foods containing large quantities of water, little change in T_g of foods is observed when water content is increased (Fig. 1). Adding water increases the free volume among food molecules and results in molecular relaxation in the system [153]. In comparison with food solids, water exhibits a small molecular weight and a low T_g (−135 °C) [84] and therefore depresses the total T_g of food systems. However, water reacts with individual food macromolecules differently. For example, carbohydrates and proteins are hydrophilic, while lipids are hydrophobic and immiscible with water. Other common plasticizers added to foods are glycerol, sorbitol and low molecular weight sugars such as glucose and fructose. The effects of other plasticizers are less significant than that of water [140]. High molecular weight additives compatible with the food solids are added to increase the T_g of foods.

Water plasticization effects and therefore the stability of foods during processing and storage may be predicted by selected models. The Gordon–Taylor equation [75] is most commonly used for experimental data. For binary food systems such as food solids and water, Gordon–Taylor equation is expressed as

$$T_{gm} = \frac{X_s T_{gs} + kX_w T_{gw}}{X_s + kX_w} \quad (1)$$

T_{gm}, T_{gs} and T_{gw} of aqueous binary mixtures are the glass transition temperatures of the mixture, solids and water, respectively; X_w and X_s are the water (w.b.) and total solids contents, and k the Gordon–Taylor parameter. The curvature of glass transition temperature–solids content relationship is described by k, denoting the strength of interaction between water and the foods solids [48]. A larger k for a binary mixture indicates that the solids are more plasticized by water than food mixtures with a smaller k and equivalent water content. Increases in k in the Gordon–Taylor model indicate greater plasticization for an equivalent amount of water, presenting a decrease in glass transition temperature. If $k = 1$, the glass transition temperature–solids content relationship is a straight line. If $k > 1$, the nature of the graphical relationship between glass transition temperature and solids content is more concave, and for $k < 1$, the nature of the relationship is convex. Starches exhibit a smaller k than sugar or food proteins, and in some instances, $k < 1$. The shape of the glass transition temperature–water content relationship is dependent on k and on the structure and composition of the solids in food systems. According to free volume theory [102], $k = \Delta\beta_{gs}/\Delta\beta_{gw}$, where β is the free volume expansion coefficient and the subscripts s and w represent solids and water, respectively. The model parameters (k and T_{gs}) of Eq. (1) are estimated using nonlinear regression analysis, where $T_{gw} = -135$ °C. At any water concentration in a binary mixture, the Gordon–Taylor model is used to calculate the glass transition temperature of the mixture, if the values of T_{gs} and k are available. For instance, the T_{gs} and k values of glucose–water solution are 31 °C and 4.07, respectively [211]. Using the Gordon–Taylor equation (1), the glass transition temperature of the glucose–water solution containing a water concentration of 0.1 is calculated as −20.7 °C. Mixtures containing more than two components may not be calculated with the Gordon–Taylor equation because a large number of experiments are necessary for adequate data collection.

The Couchman and Karasz equation [44] is based on the thermodynamic theory used to explain water plasticization in food systems. The parameter k in the Gordon–Taylor model is equivalent to the ratio of the change in specific heats of the components of binary mixture i.e., water (C_{pw}) and food solids (C_{ps}), from a thermodynamic standpoint. The Couchman and Karasz equation (2) is similar to the Gordon–Taylor equation with the parameter $k = \Delta C_{pw}/\Delta C_{ps}$.

$$T_g = \frac{X_s \Delta C_{ps} T_{gs} + X_w \Delta C_{pw} T_{gw}}{X_s \Delta C_{ps} + X_w \Delta C_{pw}} \quad (2)$$

This equation is used to calculate the glass transition temperature of the mixture, if the ΔC_p values of the components are available. For instance, the ΔC_p values of glucose and water in a mixture are 0.58 and 1.94 J/g °C, respectively [211]. Using the Couchman and Karasz equation, the glass transition temperature of the glucose–water mixture containing a water concentration of 0.1 is calculated as −13.9 °C. Unlike the Gordon–Taylor equation, the Couchman and Karasz equation can be used to predict the behavior of glass transition temperature–solids content relationship for multicomponent mixtures.

Cuq and Lcard-Verniere [46] used the Kwei equation successfully to explain water plasticization phenomena in wheat semolina. However, the Kwei equation (Eq. 3) is mainly used to model the water plasticization behavior in sugar-rich foods such as fruits (Table 1). The Kwei equation is also similar to the Gordon–Taylor equation, with the addition of one more component (qX_wX_s), indicating specific interactions in food systems or the interactions of water molecules with solids in heterogeneous food systems [129]. The Kwei equation is

$$T_{gm} = \frac{X_s T_{gs} + kX_w T_{gw}}{X_s + kX_w} + qX_s X_w \quad (3)$$

where the parameter q is a constant representing the effect of intermolecular forces such as hydrogen bonding present in a heterogeneous mixture or heterogeneous formations of food systems of large water concentrations [46, 108, 129]. A value of $q > 0$ indicates that water–food solids interactions are strong compared to solid–solid interactions, while $q < 0$ indicates solid–solid interactions are prominent, resulting in immiscibility of water in the food matrix [121].

Melting/Freezing Curve

A melting/freezing curve, representing melting/freezing point depression with an increase in solids content, is plotted as one of the main components of a state diagram of food systems. Differential scanning calorimetry and cooling curve methods are commonly used for determination of the melting/freezing point. In the case of DSC determinations, the temperature at which the last ice crystals in the food systems are melted when cooled down to an adequately low temperature ($<T_m' \sim -60$ °C for fruits) is designated as the ice-melting temperature (T_m), and the temperature at which melting of the first crystals occurs is

Table 1 Glass line and melting curve data of sugars and sugar systems

Product	Glass line				Freezing curve		References
	T_g' (°C)	X_s' (kg dry solids/kg food)	G-T model parameter T_{gs} (°C)	G-T model parameter k	T_m' (°C)	X_s' (kg dry solids/kg food)	
Arabinose	−66	0.793	−2	3.55	−53	0.793[a]	Roos [161]
Ribose	−67	0.814	−20	3.02	−53	0.814[a]	Roos [161]
Xylose	−65	0.789	6	3.78	−53	0.789[a]	Roos [161]
Fructose	−57	0.825	5	3.76	−46	0.825[a]	Roos [161]
Fucose	−62	0.784	26	4.37	−48	0.784[a]	Roos [161]
Galactose	−56	0.805	30	4.49	−45	0.805[a]	Roos [161]
Glucose	−57	0.8	31	4.52	−46	0.800[a]	Roos [161]
Mannose	−58	0.801	25	4.34	−45	0.801[a]	Roos [161]
Rhamnose	−60	0.828	−7	3.4	−47	0.828[a]	Roos [161]
Sorbose	−57	0.810	19	4.17	−44	0.810[a]	Roos [161]
Maltitol	−47	0.829	39	4.75	−37	0.829[a]	Roos [161]
Sorbitol	−63	0.817	−9	3.35	−49	0.817[a]	Roos [161]
Xylitol	−72	0.802	−29	2.76	−57	0.802[a]	Roos [161]
Glucitol	−63	0.817	−9	3.35	−49	0.817[a]	Roos [161]
Lactose	−41	0.813	101	6.56	−30	0.813[a]	Roos [161]
Lactose	−28	0.592	–	–	–	–	Slade and Levine [200]
Maltose	−42	0.816	87	6.15	−32	0.816[a]	Roos [161]
Maltose	−29.5	0.8	–	–	–	–	Slade and Levine [200]
Melibiose	−42	0.817	85	6.1	−32	0.817[a]	Roos [161]
Melibiose	−30.5	–	–	–	–	–	Slade and Levine [200]
Sucrose	−46	0.817	62	5.42	−34	0.817[a]	Roos [161]
Sucrose	−32	0.641	–	–	–	–	Slade and Levine [200]
Trehalose	−40	0.816	100	6.54	−30	0.816[a]	Roos [161]
Trehalose	−29.5	0.833	–	–	–	–	Slade and Levine [200]
Sucrose	−46	0.800	65	4.9	−35	–	Singh and Roos [196]
Sucrose/albumin (1:1)	−50	0.810	121	8.5	−30	–	
Sucrose/gelatin (1:1)	−54	0.760	95	5.9	−26	–	
Sucrose/corn starch (1:1)	−48	0.760	83	4.9	−25	–	
Sucrose/gelatin/corn starch (1:1:1)	−49	0.760	124	6.2	−24	–	

Table 1 continued

Product	Glass line				Freezing curve		References
	T_g' (°C)	X_s' (kg dry solids/kg food)	G-T model parameterT_{gs} (°C)	G-T model parameter k	T_m' (°C)	X_s' (kg dry solids/kg food)	
Dried banana	–	–	Two glass transition temperatures were detected. $T_{gs1} = 46 \pm 1$ and $T_{gs2} = 0 \pm 1$	$k_1 = 1.6 \pm 0.2$ and $k_2 = 0.9 \pm 0.1$	–	–	Katekawa and Silva [101]
Dates[b]	−50	0.70	57.4	3.2	–	–	Kasapis et al. [96]
Fructose	−48	0.790	–	–	–	–	Ablett et al. [3]
Air dried apple at 30 °C	–	–	−8.7	2.6	–	–	Welti-Chanes et al. [217]
Air dried apple at 60 °C	–	–	−1.9	3.6	–	–	
Freeze-dried apple	–	–	−13.3	2.7	–	–	
Freeze-dried apple juice	–	–	−16.3	2.4	–	–	
Freeze-dried raspberry	−61.6	0.780	42.6	4.73	−38	0.780	Syamaladevi et al. [201]
Freeze-dried pineapple	−51.6	–	57.9	0.21	−52	0.700	Telis and Sobral [204]
Dried apple slices	For food containing non-freezable water $T_g' = -55.08$	0.736	For food containing non-freezable water $T_{gs} = 41.3$	3.59	−50.3	–	Bai et al. [9]
	For food containing freezable water(without annealing), $T_g' = -59.7 \pm 1.7$		For food containing freezable water (without annealing), $T_{gs} = 70.07$	1.5			
Freeze-dried plums	−57.5	–	102.7	3.76	–	–	Telis et al. [206]
Fresh and freeze-dried Chinese gooseberry	−57.2	–	23.2	5.72	−41.8	–	Wang et al. [215]
Freeze-dried garlic	−38.6	–	40.1	3.7	−24	–	Rahman et al. [144]
Freeze-dried apple	–	–	−1.70	2.34	–	–	del Valle et al. [51]
Freeze-dried camu camu	−58.8 °C and −40.1 °C for natural pulp and pulp with maltodextrin, respectively		74.59 for natural fruit 125.45 for fruit with 30% maltodextrin	3.92 for natural fruit 5.52 for fruit with 30% maltodextrin	–	–	Silva et al. [192]
Freeze-dried and air dried tomato	−59 ± 3 for freeze-dried tomato	0.59	330.9 142.7	9.35 for freeze-dried and 6.10 for air dried tomato with osmotic pretreatment	–	–	Telis and Sobral [205]

Table 1 continued

Product	Glass line				Freezing curve		References
	T_g' (°C)	X_s' (kg dry solids/kg food)	G-T model parameterT_{gs} (°C)	G-T model parameter k	T_m' (°C)	X_s' (kg dry solids/kg food)	
Freeze-dried onion, grape and strawberry	−58.3 for onion −50.3 for grape −50.1 for strawberry	0.751 for onion, 0.803 for grape and 0.816 for strawberry		4.3, 3.3 and 4.0 for onion, grape and strawberry, respectively	–	–	Sa and Sereno [175]
Date flesh	−46.4	0.762	63.8	4.0	−43.6	–	Rahman [143]
Freeze-dried strawberries	–	–	34.2	3.52	–	–	Khalloufi et al. [103]
Freeze-dried blueberries	–	–	22.0	4.0	–	–	
Freeze-dried raspberries	–	–	47.8	2.85	–	–	
Freeze-dried blackberries	–	–	40.2	4.12	–	–	
Spray-dried tomato pulp	–	–	139.8	6.69	–	–	Goula et al. [77]
Honey	−60.5 for tree honey from Germany −62.5 for and mixed floral honey from Hungarian source	–	–	–	–	–	Kantor et al. [92]
Honey	–	–	15	3.14	–	–	Lazaridou et al. [114]
Surimi-trehalose mixture	–		123	5	–	–	Ohkuma et al. [136]
Trehalose	–	–	107	6.5	–	–	Roos [163]
Water extractable arabinoxylans (WEA)	−17 for high molecular weight and −35 for low molecular weight	–	–	–	–	–	Fessas and Schiraldi [61]
Maltose	−41	0.825[c], 0.752[d]	87	6	−31	0.825[a]	Roos and Karel [158]
Maltodextrins with different dextrin equivalents (DE)							
M365	−43	0.794[c], 0.781[d]	100	6	−28	0.794[a]	
M200	−31	0.797[c] 0.787[d]	141	6.5	−19	0.797[a]	
M100	−23	0.811[c], 0.781[d]	160	7	−13	0.811[a]	
M040	−15	0.729[c], 0.794[d]	188	7.7	−11	0.729[a]	

[a] X_s' and X_s'' are equivalent in the study

[b] Rheological test under low amplitude oscillatory shear

[c] From Gordon–Taylor model

[d] From extrapolated ΔH_m values

designated as the onset of ice melting (T_m'). When considering the freezing temperature of water to ice in food systems, as in the case of the cooling curve method, the initial crystallization temperature is designated as the initial freezing point (T_F). This is located as the onset of ice crystallization, where there is an abrupt increase in temperature due to the release of latent heat [148]. In the cooling curve method, T_m' is designated as the endpoint of freezing. At the melting/freezing point, the vapor pressure of the solid and liquid are equal, and both phases exist in equilibrium. The freezing point of water or the melting point of ice is an equilibrium process, where neither cooling nor heating rate affect the phase transition point of ice crystallization. Like the glass line, the nature of melting/freezing curve is strongly dependent on food composition. Moreover, the T_m' as well as the glass transition temperature of the maximum-freeze-concentration solution (T_g') is identified with a melting/freezing curve.

Characterizing Melting/Freezing Temperature

A differential scanning calorimetry method is used extensively to characterize the onset of ice melting (T_m') and the decrease in melting temperature ice crystals, due to increasing solids content in foods [144, 148]. Thermograms provide melting endotherms and glass transition temperatures of maximum-freeze-concentrated solutions for foods containing freezable water (Fig. 9). The ice-melting temperature (T_m) of foods is taken as the peak temperature of the melting endotherm as presented in Fig. 9 [8, 72]. However, in foods with broader endotherms, a tangent to the left side of the melting endotherm curve is plotted. T_m is identified as the point where maximum slope of the endotherm is observed [9, 143, 150]. However, the DSC is conducted with only a small quantity of food sample and may not represent actual melting scenarios, since foods are complex mixtures of various components [148].

Use of the cooling curve method to determine initial freezing temperature (T_F) is simple and inexpensive compared to the DSC method. Complex and multicomponent food systems may not be completely represented by the small food quantity of 5–15 mg in the DSC [148]. Initial freezing temperature (T_F) and T_m' can be precisely determined with the cooling curve method [148]. In the cooling curve method, a metallic cylinder containing the food system is placed in a freezer maintained at low temperatures (<−60 °C). The temperature at the geometric center of the food sample is determined at selected time intervals using a thermocouple. Figure 10 shows a typical cooling curve. The solid line represents the temperature of the material during cooling, while the dotted line represents the slope of the cooling curve. At point *a* (onset of ice crystallization), temperature abruptly increases due to the release of latent heat to point *b*, which is considered the

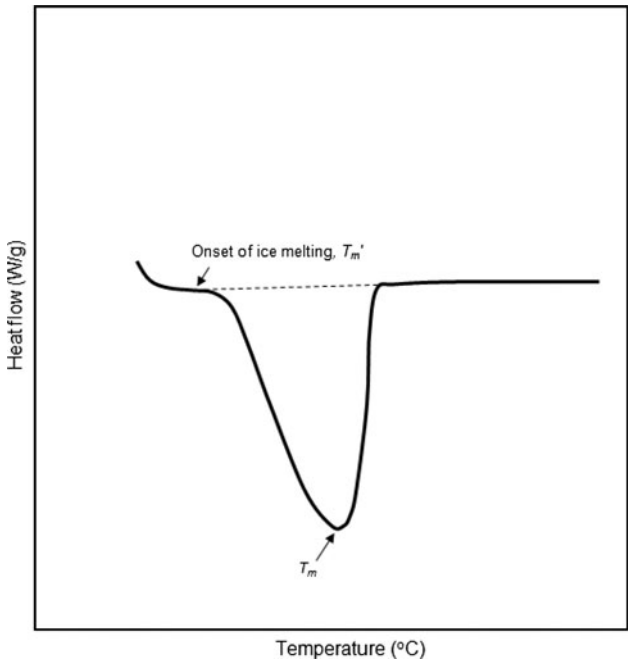

Fig. 9 A typical DSC thermogram of food systems with freezable water presenting ice-melting temperature (T_m) taken as the peak temperature of melting endotherm and onset of ice-melting temperature (T_m') taken as the intersection point of the baseline with the left side of the endotherm

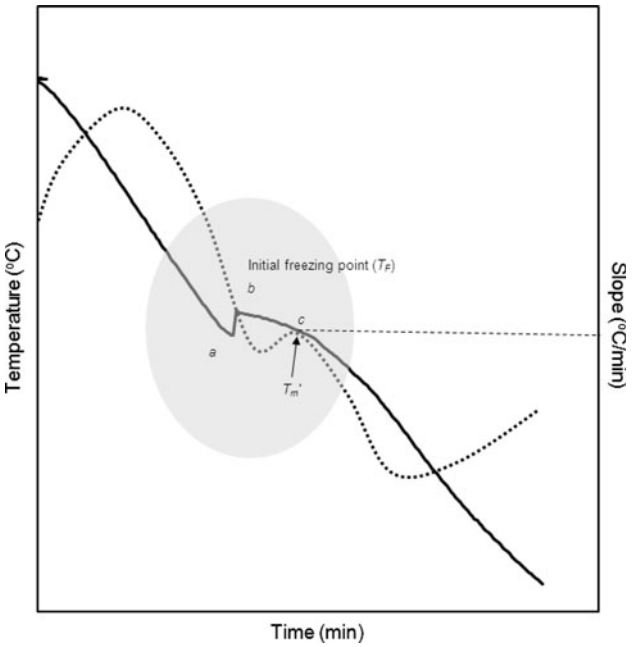

Fig. 10 A typical cooling curve presenting initial freezing point (T_F) and onset of ice melting (T_m'). At point *a*, sudden increase in the temperature due to the release of latent heat to point *b*, considered the initial freezing temperature (T_F). At point *c*, greatest slope of the cooling curve is observed, which is considered as the onset of ice melting (T_m')

initial freezing temperature (T_F). At the initial freezing temperature, the slowest cooling rate is observed. The cooling curve method was used to obtain the freezing curve of dates [96], garlic [144], abalone [177] and tuna flesh [146]. This method can be used for solids, liquids and viscoelastic materials. The cooling curve method is relatively inexpensive, and sample preparation is relatively easy [148]. However, the cooling curve method is less accurate when materials contain smaller amounts of freezable water [148].

Characterizing Conditions of Maximum-Freeze-Concentration Solutions

The crystallization of water in foods occurs at temperatures lower than 0 °C, since freezing temperature depression relates to the concentration of solids. As temperature is decreased and water is removed from a food in the form of ice, the solutes in the unfrozen water are freeze concentrated. An increase in the viscosity of the unfrozen phase occurs, thus decreasing the diffusion properties of the system and hindering additional ice crystallization. This highly concentrated unfrozen solution goes through a glass transition if temperature is decreased further. Maximum-freeze-concentrated conditions in foods correspond to maximum ice formation at low temperatures. These conditions are characterized by two temperatures: the onset of ice melting (T_m') and the glass transition temperature for maximum-freeze-concentration (T_g'), both which are lower than 0 °C. At T_m', the viscosity of the maximum-freeze-concentrate lies in the range of 10^7 Pas [157]. The difference between T_m' and T_g' is often very small, and the two temperatures may coincide for high molecular weight food components [164]. The water content corresponding to T_g' is the unfrozen water. T_m' and T_g' also increase with increasing molecular weight of food components.

The ice formation in freeze-concentrated solutions is time-dependent, and therefore determination of characteristic temperatures (T_m' and T_g') of freeze-concentrated solutions is challenging. It is difficult to observe small changes in unfrozen water associated with ice melting at temperatures close to T_m' [183]. Thermograms of foods with high water content generally exhibit multiple transitions, and the lower transition temperature is commonly assigned as T_g' [2, 159]. However, the assignment of T_m' and T_g' of maximally freeze-concentrated solutions is a subject of debate [24, 63, 73, 153]. The complex behavior of maximally freeze-concentrated solutions is attributed partly to the excess enthalpy resulting from the molecular relaxations near T_g' [73]. Generally, the onset temperature of ice melting (T_m') is determined by plotting a base line linear to the endotherm. The intersection point of the baseline with the left side of the endotherm is defined as the T_m' (Fig. 9). Annealing is performed at a temperature ($T_m'-1$) for systems containing freezable water, allowing maximum ice formation to avoid the crystallization endotherm. Annealing time must be optimized to achieve maximum-freeze-concentrated solutions. After annealing, the foods are cooled from ($T_m'-1$) to a low temperature and scanned to a preselected temperature range depending on the food system. The T_m' and T_g' are determined from a single thermogram. However, accuracy of this technique may depend on selected factors, such as heating and cooling rates or annealing conditions [148]. Also, the value of T_m' is dependent on the intersection point of the baseline with the left side of the endotherm [63]. A state diagram may be better utilized to assess the temperatures and states of the food system at maximum-freeze-concentration conditions. The value of T_g' for a specific food is normally determined by extending the freezing curve to the glass line in a state diagram, as presented in Fig. 1. However, T_g' observed using the results from DSC analysis may be considerably different from the T_g' determined from state diagram [24, 201]. A procedure similar to the initial freezing point determination is followed to identify the onset of ice melting (T_m'), using the cooling curve method. At point *c* (Fig. 10), the slope of the cooling curve changes and a maximum cooling rate is observed. Point *c* is regarded as the onset of ice melting (T_m'). The T_m' obtained with the cooling curve method is comparable to that determined with DSC [148]. However, the cooling curve method for determination of T_m' is less sensitive than DSC for concentrated foods [144].

An approach similar to the determination of the glass transition temperatures of low-moisture food systems, mechanical analysis with annealing at temperatures below T_m' may be used to determine the glass transition temperatures of high-moisture foods (T_g'). At glass transition temperatures (T_g'), a maximum value of E' (or G'), E'' (G'') and tan δ of foods is observed. Melting temperatures of ice also may be obtained with DMTA. The peak in the value of E' (or G') at a high temperature represents the melting of ice, while the peak in the value of E' (or G') at a low temperature represents the T_g of food solids [111]. DEA/DETA is considered a more sensitive method to determine T_g' than DSC or DMA. In dielectric techniques, the dielectric constant or permittivity (ε') expresses the degree of alignment of dipole molecules to the electric field. The dielectric loss factor (ε'') expresses the energy needed to align the dipole molecules. The tan δ ($=\varepsilon''/\varepsilon'$) of foods is a function of temperature/frequency for an applied stress and is detected by alternating current [151]. The melting temperatures of ice and glass transition temperatures are determined using DEA. A peak in tan δ provides glass

transition temperatures at maximum-freeze-concentration conditions (T_g') [110].

Characterizing Unfrozen Water (X_w')

Unfrozen water (X_w' or $1-X_s''$) in frozen foods may result in deterioration during long-term storage due to its molecular mobility. Three different approaches may be followed to calculate the concentration of unfrozen water in frozen foods. In the first approach, the change in enthalpy during ice-melting is determined [117]. Using Eq. 4, the area under the ice-melting endotherm is determined and the quantity of unfrozen water (X_w') is calculated.

$$X'_w = X^0_w - \frac{(\Delta H_m)_{\text{frozen food}}}{(\Delta H_m)_{\text{water}}} \tag{4}$$

where X^0_w is the water content of the frozen food $(\Delta H_m)_{\text{frozen food}}$ is the change in enthalpy during melting of ice in the frozen food and $(\Delta H_m)_{\text{water}}$ is the change in latent heat of melting of ice (334 kJ/kg).

A second approach is to plot the linear relationship between $(\Delta H_m)_{\text{frozen food}}$ and the water content of annealed high-moisture foods [193]. The unfrozen water is considered the water content corresponding to $(\Delta H_m)_{\text{frozen food}} = 0$. The most common and reliable approach for the determination of unfrozen water is to extend the freezing curve to the glass line of the food system on a state diagram following the curvature of the freezing curve [3, 67]. The temperature and water concentration at the intersection point of the glass line and the freezing curve are considered as T_g' and the quantity of unfrozen water, respectively (Fig. 1). The accuracy and utility of the three approaches for the determination of unfrozen water is discussed in the literature [24, 63, 143]. The unfrozen water quantities obtained by the three approaches vary depending on the assignment of onset or midpoint glass transition temperatures in the thermograms [24]. Also, the assignment of melting and glass transition temperatures determines the quantity of unfrozen water [24, 63]. Blond et al. [24] attributed the difficulty in defining a true intersection between the freezing curve and the glass line to differences in the onset and midpoint glass transition temperatures. Studies relating molecular mobility and viscosity of the unfrozen phase to diffusion-induced mechanisms may provide a better understanding of T_g' and unfrozen water in frozen food systems [24].

Characterizing the Effects of Solids Content on Equilibrium Melting Temperature

A number of empirical and theoretical models are available for relating the equilibrium melting/freezing temperatures with solids content of food biopolymers [141]. The Clausius–Clapeyron equation and the Chen equation are used extensively to predict equilibrium melting temperatures of selected food systems. The Clausius–Clapeyron equation (5)

$$\delta = -\frac{\beta}{\lambda_w}\ln\left[\frac{1-X_s}{1-X_s+EX_s}\right] \tag{5}$$

where δ is the melting/freezing temperature depression relative to increasing total solids concentration, β is the molar freezing temperature constant for water (1,860 kgK/kg mol), λ_w is the molecular mass of water, X_s is the solids mass fraction in a food system, and E is the molecular mass ratio of water to solids (λ_w/λ_s).

The Clausius–Clapeyron equation is applicable to ideal systems, but multicomponent systems are normally non-ideal in nature. The Chen equation [35] is an extension of the Clausius–Clapeyron equation and may be used to predict the freezing temperature for non-ideal systems. The Chen equation (6) is expressed as:

$$\delta = -\frac{\beta}{\lambda_w}\ln\left[\frac{1-X_s-BX_s}{1-X_s-BX_s+EX_s}\right] \tag{6}$$

where a new parameter B, the ratio of unfrozen water to the total solids concentration, and the parameter E are estimated using nonlinear optimization analysis.

A set of theoretical equations (7–11) was developed to predict the T_g' and corresponding solids content X_s'' on a state diagram for aqueous solutions of mono-, oligo- and polysaccharides. These are derived from standard glass transition temperatures of anhydrous solids and specific heat changes for mixtures of pure solids and water based on a water clustering model [127].

$$\frac{T_{gw}}{T'_g} = 1 - 0.145f(y) \tag{7}$$

$$X'_s = 0.55z(2.645-y)^{0.5} \tag{8}$$

The function $f(y)$ and y are calculated from following equations using iterative procedures.

$$6.896K_2(z-1)z = (zK_2-1)zf(y) + \phi(y) \tag{9}$$

$$f(y) = \ln(2y^{1.5}((1.55y^{0.5}-1)^3 + 1/3)) \tag{10}$$

$$\phi(y) = 1.819f(y)(2.645-y)^{-0.5} \tag{11}$$

where $z = T_{gs}/T_{gw}$ and $K_2 = \Delta C_{ps}/\Delta C_{pw}$These equations were further modified to accurately calculate T_g' and X_s'' values for frozen aqueous solutions of proteins and solutions of polysaccharides [128].

State Diagram Data

The following sections discuss the Gordon–Taylor equation constants (T_{gs} and k) obtained from glass transition

temperature–solids content relationships (glass line), Chen equation constants (E and B) obtained from melting/freezing point–solids content relationships (melting/freezing curve), and conditions of maximum-freeze-concentrations (T_g', T_m' and X_w') of foods. Tables 1, 2, 3, 4 and 5 present the state and phase transition data.

Sugars

Studies of glass transitions and applications are more often conducted for sugars than for starches or proteins. In fruits, glass transitions are detected due to the presence of sugars including glucose, fructose and sucrose. State diagrams of fruits are similar to their major amorphous components. State diagram data (T_g', T_m', T_{gs} and k values) of monosaccharide and disaccharide solutions and selected fruit solids are presented in the literature [141, 160]. Calorimetric methods are widely used for development of the state diagrams of sugars (Tables 1). Glass transition temperatures in amorphous sugars are easily detected by DSC. Single and narrow range glass transition temperatures are commonly observed for fruit solids and attributed to compatible and simple structures. The Gordon–Taylor equation and the Kwei equation are commonly used to characterize the plasticization effect of water on sugars. Glass transition temperatures of dry fruit solids (T_{gs}) range from −29 to 107 °C and from −16.3 to 142.7 °C for sugars and fruit solids, respectively (Table 1). The T_{gs} of fruit solids (mainly sugars) are smaller than the T_{gs} of food protein or starch because of differences in molecular weight. Within sugars, trehalose exhibits a high T_{gs} (100 °C), which is attributed to high molecular weight. Maltose and lactose also exhibit high glass transition temperatures (T_{gs}). However, high molecular weight may not be the sole cause of high anhydrous glass transition temperatures. For instance, glucose and fructose exhibit equivalent molecular weights and their T_{gs} are 31 and 5 °C, respectively (Table 1). Normally, fruit solids exhibit large k values, indicating that sugars are easily plasticized by water. The k values of pure sugars range from 3.02 to 6.56, while fruit solids exhibit k values ranging from 0.21 to 6.69. Trehalose and lactose exhibit larger k values than other pure sugar components. The larger k value (4.52) for glucose compared to the k value (3.76) of fructose also exhibits a greater decrease in glass transition temperatures with small additions of water compared to fructose.

Chen and Clausius–Clapeyron equations are used to fit the melting/freezing point depression of fruits. The parameter E in Chen and Clausius–Clapeyron equations relates to the molecular mass ratio of water to solids (λ_w/λ_s). The value of E is dependent on the type of food solids. For instance, date flesh consists of approximately 75% of a solids mixture of sucrose, glucose and fructose. The mean molecular weight of the food solids of dates obtained from the parameter E is 200 (Table 1). The constant B in the Chen equation presents the ratio of unfrozen water to total food solids. The constant B only provides an approximate value of unfrozen water. The values of E ranged from 0.064 to 0.129 for selected fruits, while B values ranged from −0.062 to 0.429. The negative value of B indicates that a fraction of solids is behaving as a solvent. Chen [35] indicated that melting/freezing point depression results from the complex interaction between solutes and water and can be expressed by equivalent increases in free water. Thus, the values of B can either be positive or negative depending on the behavior of food constituents.

The T_g' of freeze-concentrated solutions of fruit solids range from −60 to −40 °C, while the T_m' range from −52 to −24 °C (Table 1). T_g' and T_m' of small molecular weight sugars as well as fruit solids are lower than the T_g' and T_m' of proteins and starches (Table 1). Dissimilar values of T_g' and T_m' for pure sugars may be attributed to experimental conditions and methods. The T_m'–T_g' of fruit solids range from 0.4 to 15 °C. Normally, fruit solids consist of more unfrozen water than starch or protein-rich foods. The unfrozen water content of selected sugars ranges from 0.172 to 0.535 kg water/kg sugars. A state diagram of amorphous sucrose is presented in Fig. 11. Amorphous sucrose may be prepared by many methods, including freeze-drying [169]. The variation in glass transition temperature (T_g) and ice-melting temperature (T_m) of amorphous sucrose solutions with solids content are presented as a glass line and melting curve in the state diagram [159]. Figure 12 presents a state diagram of raspberry solids. Here, the glass line and melting curves are modeled using Gordon–Taylor and Chen equations, respectively. [201].

Starches

Calorimetric and mechanical determinations are often used to study the glass transition of starch systems (Table 2). Both the Gordon–Taylor and Couchman–Karasz equations are used to model the plasticization influence of water on starches. The T_g of high molecular weight starches are relatively higher than the T_g of sugars. T_{gs} of selected starches range from 75 to 281 °C (Table 2). High glass transition temperatures (T_{gs}) of starches may be attributed to biopolymer interactions, limiting molecular motion and increasing molecular rigidity and viscosity. The T_g increases with an increase in molecular weight, occupied volume, rigidity, polarity of side chain groups, covalent and non-covalent bonds and cross-linkages among biopolymers [53]. Moreover, as molecular weights increase, the cross-linking density of biopolymers increases the stiffness of the biopolymers, reducing the mobility and increasing T_g of

Table 2 Glass line and melting curve data of starch systems

Product	Glass transition curve				Freezing curve		References
	T_g' (°C)	X_s'(kg dry solids/kg food)	G-T model parameter T_{gs} (°C)	G-T model parameter k	T_m' (°C)	X_s'(kg dry solids/kg food)	
Extruded wheat	–	–	281	–	–	–	Bindzus et al. [22]
Extruded corn			281		–	–	
Extruded rice starch			281		–	–	
Corn starch	−11	0.730	243	5.6	−11	0.730	Jouppila and Roos [86]
Yellow corn cakes	–	–	128 for yellow corn cakes	2.58 for yellow corn cakes	–	–	Li et al. [118, 119]
White corn cakes	–	–	115 for white corn cakes	2.39 for white corn cakes	–	–	
Gelatinized waxy corn starch	−6	0.730	–	–	−6	–	Roos and Karel [158]
Gelatinized corn starch	–	–	277.8	5.7	–	–	Zhong and Sun [225]
Gelatinized wheat starch	−5	0.730	–	–	−5	–	Slade and Levine [198]
Wheat semolina[a]	–	–	T_{gs} values are 162, 176 and 225 for heating, cooling and reheating, respectively	k values are 3.4, 4.2 and 5.5, respectively for heating, cooling and reheating, respectively	–	–	Cuq and Lcard-Verniere [46]
Cooked rice stick noodles	−4.0	–	–	–	–	–	Israkarn and Charoenrein [83]
Amylopectin–water mixture[b]	−7	0.715	227	4.0	–	–	Brent et al. [28]
Zein–water mixture	−48.0	0.815	137	–	–	–	
Extruded corn meal	−3	0.700	–	–	–	–	
Native corn starch	−6.6	–	–	–	–	–	Chung et al. [40]
Pea starch (Amylose:Amylopecin = 2:1)[c]	–	–	75	–	–	–	De Graaf et al. [49]
Potato starch (Amylose:Amylopecin = 1:4)	–	–	152	–	–	–	
Wheat starch (Amylose:Amylopecin = 1:4)	–	–	143	–	–	–	
Waxy maize (Amylose:Amylopecin = 1:99)	–	–	158	–	–	–	
Starch-based wafers	–	–	133	5.54	–	–	Martinez-Navarrete et al. [125]
Rice[d]	−11.6	–	158.5	6.38	−3.6	0.600	Sablani et al. [182]

[a] MDSC

[b] DSC and DMTA

[c] DMTA

[d] Cooling curve

Table 3 Glass line and melting curve data of plant proteins

Product	Glass curve				Freezing curve		References
	T_g' (°C)	X_s' (kg dry solids/kg food)	G-T model parameter T_{gs} (°C)	G-T model parameter k	T_m' (°C)	X_s' (kg dry solids/kg food)	
Native wheat gluten[a]	–	–	173 for native gluten	5.10 for native gluten	–	–	Micard and Guilbert [129]
Hydrophobized wheat gluten			174 for hydrophobized gluten	4.69 for hydrophobized gluten			
gliadin and glutenin-rich fractions			162 for gliadin-rich fractions	4.48 for gliadin-rich fractions			
			175 for glutenin-rich fractions	5.26 for glutenin-rich fractions			
Wheat gluten plasticized with water, glycerol and sorbitol[b]	–	–	187 for that plasticized by water,	4.85 for that plasticized by water,	–	–	Pouplin et al. [140]
			187 for that plasticized by glycerol	2.2 that plasticized by glycerol,			
			187 for that plasticized by sorbitol	2.4 for that plasticized by sorbitol by Couchman–Karasz model			
Gliadin[b]	–	–	121.4	3.6	–		De Graaf et al. [48]
High molecular weight glutenin	–	–	139	5	–	–	Noel et al. [135]
Alkylated glutenin			138	4.3			
α-gliadin			144	4.6			
γ-gliadin			124	3.8			
ω-gliadin			145	4.2			
Gluten[b]	–	–	162	0.2	–	–	Kalichevsky et al. [90]
Wheat gluten[c]	–20	0.760	127.6 ± 4.1	3.9 ± 0.24	–	–	Toufeili et al. [210]
Green peas	−26 for young green peas	–	–	–	–		Lim et al. [120]
	−20 for old green peas						
Soy globulin (7S and 11S)	−67 for 7S globulin	–	114 and 6.72	6.72	–	–	Morales and Kokini [131]
			160 and 6.66	6.66			
	−17 for 11S globulin						
Gluten	–	–	161.9 and 4.93	4.93	–	–	Bengoechea et al. [16]
Soya protein			172.0 and 4.42	and 4.42			
Sunflower protein	–	–	179	5.16	–	–	Rouilly et al. [171]
Zein	–	–	139	6.24	–	–	Madeka and Kokini [123]

[a] MDSC

[b] DMTA

[c] Mechanical spectrometry and pressure rheometry

Table 4 Glass line and melting curve data of animal proteins

Product	Glass line				Freezing curve		References
	T_g' (°C)	X_s' (kg dry solids/kg food)	G-T model parameters T_{gs} (°C)	G-T model parameters k	T_m' (°C)	X_s' (kg dry solids/kg food)	
Chicken meat	−16.8	0.924	–	–	–	–	Delgado and Sun [50]
Myofibrillar proteins[a]	–	–	235	6.06	–	–	Cuq et al. [45]
Casein and Sodium Caseinate[a]	–	–	144 for casein 130 for Sodium Caseinate	0.43 for casein 0.76 for Sodium Caseinate	–	–	Kalichevsky et al. [91]
Mackerel	−13.3 ± 0.5	–	–	–	–	–	Brake and Fennema [27]
Cod	−11.7 ± 0.6	–	–	–	–	–	
Beef muscle	−12.0 ± 0.3	–	–	–	–	–	
King fish muscle	T_g' varied from −21.4 to −25.5	0.688	–	–	−17.4	0.688	Sablani et al. [181]
Tuna meat[b]	−54.2	0.61	95.1	2.89	−13.3	0.61	Rahman et al. [146]
Freeze-dried shark[b]	–	–	152	5.35	–	–	Sablani and Kasapis [178]
Abalone[b]	−44.3	0.68	–	–	−18	0.68	Sablani et al. [177]
Whole milk powder	–	–	100.6	8.57	–	–	Vuataz [214]
Skim milk powder	–	–	101	6.5	–	–	
Ovalbumin	–	–	207	–	–	–	Katayama et al. [100]
Ribonuclease A	–	–	183	–	–	–	
Hydroxyl ethyl starch	–	–	225	–	–	–	
Casein[c]	–	–	206.4	4.97	–	–	Bengoechea et al. [16]
Gelatin[b]	–	–	161	6.1	–	–	Kasapis and Sablani [97]

[a] DMTA

[b] Rheological analysis

[c] PTA

starches [208]. Starches exhibit broad glass transition temperature ranges (T_{gi}–T_{ge}) attributed to large molecular weights and incompatibility of constituents, while many small molecular weight sugars exhibit glass transitions ranges (T_{gi}–T_{ge}) of a few degrees [208]. Multiple glass transition temperatures are observed in many starch-rich foods. Perdon et al. [139] observed three apparent glass transition temperatures of rice kernels at specific water contents attributed to the structural characteristics of heterogeneous starch as well as the coexistence of the crystalline/semicrystalline and amorphous regions of starch.

Mean k values in the Gordon–Taylor equation for starches ranging from 2.39 to 6.38 are relatively smaller than the mean k values for proteins and sugars (Tables 1 and 2). Starch may absorb less water than readily plasticized hydrophilic and amorphous proteins or polysaccharides [126]. Plasticization of foods by water depends on many factors, including the hydrophilicity of the food constituents, the quantity of water in food systems and the thermodynamic compatibility of water with food constituents. Statistical models are better suited to correlate glass transition temperatures with the water or solids content. The extrapolation of the relationship to foods containing zero water provides glass transition temperatures for dry starches [22]. Extruded starches exhibit higher T_{gs} than T_{gs} of native starches. Bindzus et al. [22] reported that starches may exhibit similar states and state transitions, regardless of their botanical origin or processing conditions.

Table 5 Glass line and melting curve data of other polysaccharides/protein systems

Product	Glass line				Freezing curve		References
	T_g' (°C)	X_s'(kg dry solids/kg food)	G-T model parameter T_{gs} (°C)	G-T model parameter k	T_m' (°C)	X_s' (kg dry solids/kg food)	
Chitosan	–	–	367.9	1.68	–	–	Lazaridou and Biliaderis [113]
Starch–Chitosan mixture	–	–	363.7	1.97	–	–	
Pullulan Chitosan mixture	–	–	353.5	1.72	–	–	
Pullulan[a]	–	–	476.6 and 4.83 for DMTA 425 and 3.78 for DSC	–	–	–	Diab et al. [52]
Pullulan/sorbitol (P/S, 85:15 w/w)	–	–	422.6 and 3.55 for DMTA 375 and 3.33 for DSC				
Pullulan/sorbitol/ sucrose	–	–	373.8 and 3.08 for DMTA 332.1 and 3.12 for DSC	–	–	–	

[a] DMTA

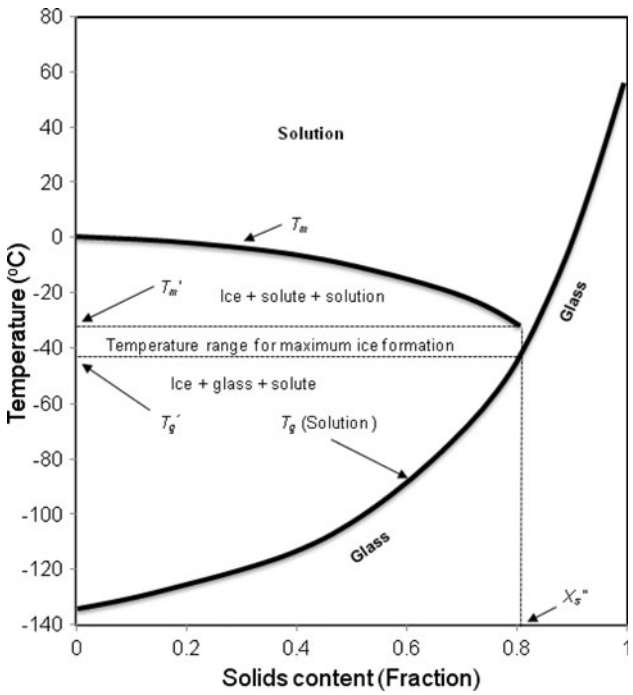

Fig. 11 State diagram of sucrose presenting glass line and freezing curve; T_m', onset ice-melting temperature in a maximally freeze-concentrated solution; T_g', glass transition temperature in a maximally freeze-concentrated solution; X_s'', solids content corresponding to T_g' (Adapted from [159])

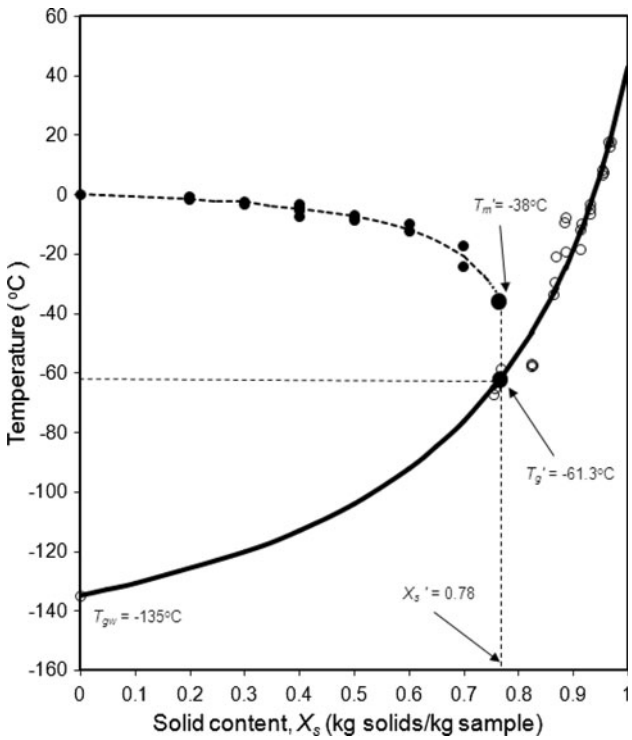

Fig. 12 State diagram of raspberry solids presenting glass line and freezing curve; T_m', onset ice-melting temperature in a maximally freeze-concentrated solution; T_g', glass transition temperature in a maximally freeze-concentrated solution (Adapted from [201])

Starches normally exist in both amorphous and crystalline states. For example, linear amylose in starch basically exhibits an amorphous structure, while amylopectin exhibits a crystalline/semicrystalline structure. The amorphous portion undergoes glassy to rubbery transitions, and the crystalline portion of the starches melts during heating. Amylopectin in waxy maize exhibits a high T_g. Amylose exhibits a lower T_g than amylopectin, attributed to the

smaller molecular mass of amylose and the smaller degree of polymerization [49]. Zhong and Sun [225] report that gelatinized corn starch exhibits a higher glass transition temperature than native corn starch. Tan et al. [203] report that the glass transition temperature of waxy maize starch overlaps with the peak gelatinization temperature attributed to the loss of crystallinity. Glass transition and gelatinization temperatures are reduced by the addition of water content. Moreover, Tan et al. [203] report that the addition of glycerol to maize starch increases the glass transition and gelatinization temperatures at small water contents.

Semicrystalline portions of starch may crystallize with time during storage. Storing of starch-rich foods at a temperature lower than glass transition temperatures may reduce the rate of crystallization due to the large viscosity of starches. The extent of crystallization of starches depends mainly on the difference between storage temperature and the glass transition temperature of the particular starch (T–T_g) [86]. Li et al. [118, 119] reported loss of crispness in glassy corn cakes. Recently, Van Nieuwenhuijzen et al. [212] reported that the loss of crispness of bread crust is more dependent on water content than water activity, though both may influence crispness. Proton mobility, representing water mobility determined by NMR, was not influenced by water activity at constant water concentrations in bread crust.

Glass transition temperatures at maximum-freeze-concentration (T_g') of starches are higher than the glass transition temperatures of sugars or proteins (Tables 1, 2 and 3). T_g' and T_m' of common mono-, di-, oligo- and polysaccharides were determined and the difference in the temperatures (T_m'–T_g') ranged from 10 to 15 °C. (T_m'–T_g') was consistent for polysaccharides. However, little information about T_g' and X_w' of starches is available in the literature. T_g' of selected starch systems ranged from −3 to −11 °C (Table 2). Melting/freezing curves and T_m' of limited starch systems are provided in Table 2. Previously, equivalent values for T_g' and T_m' were adopted for starch systems [158]. The quantity of unfrozen water for selected starch systems ranging from 0.185 to 0.3 kg water/kg starch is in the general range for unfrozen water of many other food systems, such as proteins and fruit solids (Table 2). Unfrozen water is lowest in pure starches compared to food solids consisting of small molecular weight constituents. The semicrystalline and hydrophobic nature of starch is related to the small quantity of unfrozen water in starch-rich foods. Compared to the ordered structure of starch, proteins and sugars exhibit a hygroscopic amorphous nature and greater quantities of water adsorption than starch [104]. Figure 13 presents the state diagram of amorphous gelatinized corn starch. The glass line is modeled using Gordon–Taylor. The T_g' and T_m' values of corn

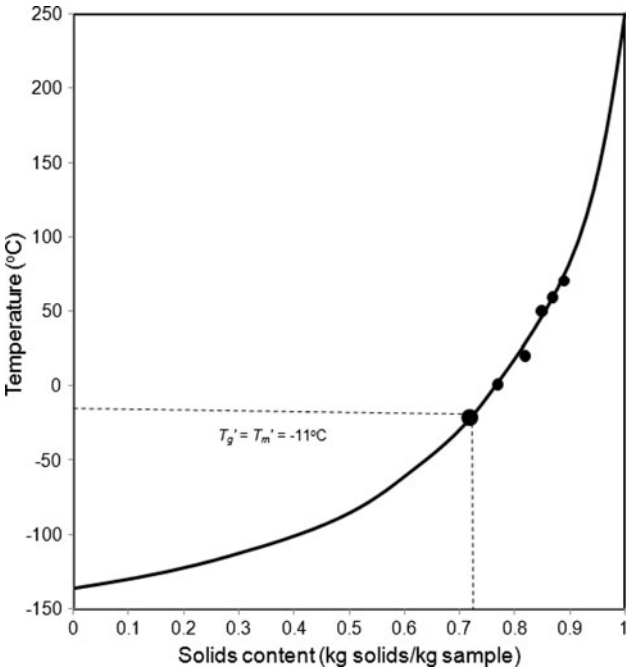

Fig. 13 State diagram of gelatinized corn starch presenting glass line; T_m', onset ice-melting temperature in a maximally freeze-concentrated solution; T_g', glass transition temperature in a maximally freeze-concentrated solution; (Adapted from [86])

starch are −11 °C, respectively, which are greater than typical values for sugars.

Plant Proteins

Proteins exhibit complex structures and large molecular weights ranging from thousands to millions. Structurally, proteins are amino acids bound by peptide linkages into long chains. Plant proteins play a major role in the human diet and are necessary for the growth of cells. Protein denaturation is sensitive to temperature changes during processing and storage. Research on state diagrams of plant proteins is concentrated on gliadin, glutenin and gluten [48, 129, 134, 135, 140]. DMTA, DSC and MDSC are the most useful methods to determine the T_g of plant proteins. Kokini et al. [104] reported that the combined use of DSC and DMTA allows researchers to study state transitions of proteins in a broad range of temperatures and water contents. State diagrams with different states (glassy, rubbery, entangled polymer flow, reaction zone and softening) of selected proteins (gliadin, zein and glutenin) are developed [104].

Like starches, glass transition temperatures of dry proteins (T_{gs}) are high, attributed to large molecular weights. Studies on glass transition in many anhydrous proteins and polysaccharides are difficult due to denaturation and decomposition of the biopolymers during heating [165].

However, the mean T_{gs} obtained for the selected plant proteins ranged from 114 to 187 °C (Table 3). The T_{gs} of plant protein-rich foods were greater than the T_{gs} of sugars and smaller than the T_{gs} of starches and animal proteins. There are inconsistencies in the T_{gs} of wheat gluten, the most studied plant protein for glass transition analysis (Table 3). This may be attributed to the choice of methods and experimental conditions. Mean k values ranging from 0.2 to 6.72 for proteins systems are greater than k values for carbohydrates or starches (Tables 1, 2 and 3). Most of the proteins are hydrophilic in nature and highly plasticized by water compared to starches. The k values of soy globulins (6.72 and 6.66 for 7S and 11S, respectively) are larger than the k values for selected plant proteins (Table 3). Micard and Guilbert [129] reported that for gluten, the value of k is between the k values of gliadin and glutenin. The smaller k values of hydrophobized gluten are attributed to less plasticization. The plasticizing effect of glycerol and sorbitol added to wheat gluten proteins is less prominent than the plasticizing effect of water [140]. Due to the smaller molecular weights and smaller concentrations of hydrophilic amino acids in gliadin, the decrease of T_g for gliadin with added water was smaller than the decrease of T_g for gluten and glutenin [48]. Plasticization of proteins by water is important, since plasticization affects the quality of protein-based edible films and food systems, and the stability of protein-rich foods during frozen storage [162].

T_m', T_g' and melting curve information for protein-rich foods is limited (Table 3). T_g' of selected plant proteins ranged from −15 to −30 °C and was higher than the T_g' of sugars and fruit solids (Tables 1, 3). Maximum-freeze-concentration conditions (T_g' and T_m') are not available for many plant protein systems. Future research is needed to develop state diagrams with melting curves and concentrations of unfrozen water in protein systems. Figure 14 presents a state diagram for zein (to water concentrations from 0 to 35%), developed using glass transition and pressure rheometry results [105].

Animal Proteins

Rheological, mechanical and calorimetric studies are conducted to analyze state transitions in animal proteins. T_{gs} values of selected animal protein foods range from 95 to 235 °C, higher than the T_{gs} of sugars (Table 4). Hashimoto et al. [81] reported the glass transition temperatures of whole fish muscle is less than the T_g of extracted proteins, probably due to the plasticizing effect of small molecular weight materials such as salts and sugars. Glass transition temperatures of dry fish proteins ranged from 130 to 180 °C. Mean k values for animal protein systems range from 0.43 to 8.57 (Table 4). Cooling curve methods are used to obtain the freezing temperature depression of

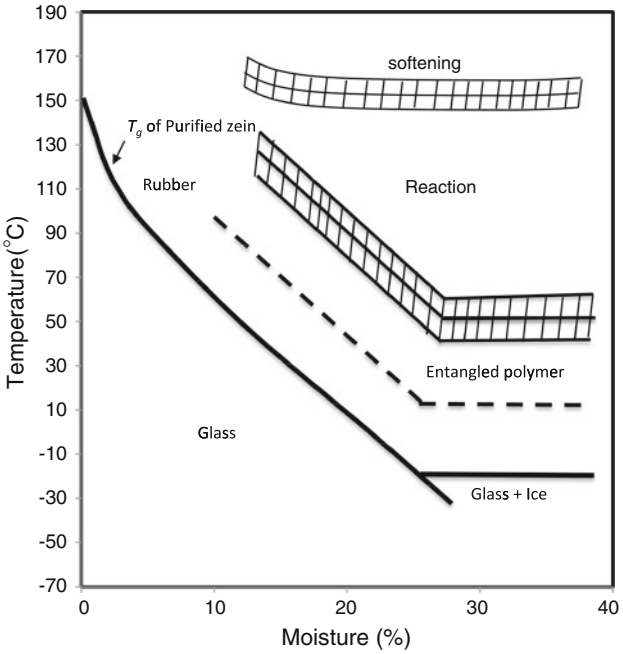

Fig. 14 State diagram of zein presenting various transitions including glass to rubber, rubber to entangled polymer flow; the increase in temperature and water results in enhancement of mobility, reaction rate and softening of zein system (Adapted from [123])

selected animal protein systems [148]. The data obtained from cooling curve methods is modeled using Chen, as well as the Clausius–Clapeyron equations in selected animal proteins [146, 177, 180]. The Chen equation parameter E ranges from 0.0275 to 0.071, while parameter B ranges from 0.303 to 0.383 for selected animal protein systems.

Generally, the T_g' of animal proteins are lower than that of plant proteins (Tables 3, 4). However, Kalichevsky et al. [91] reported that the T_g of casein is greater than the T_g of amylopectin or gluten at equivalent water content. The T_g' of selected animal proteins ranges from −44.3 to −11.3 °C, while the T_m' for selected animal proteins ranges from −18 to −13.3 °C (Table 4). The positive difference between T_g' and T_m' (T_g'–T_m') range from 4 to 40 °C in selected animal protein systems. The quantity of unfrozen water in the selected animal protein systems ranges from 0.312 to 0.390 kg water/kg protein (Table 4). However, the quantity of unfrozen water for many animal protein systems is not available. Similar to starches, broad ranges in glass transition temperatures (T_{gi}–T_{ge}) were observed in proteins, attributed to the complex molecular structure of proteins [45]. A state diagram of protein-rich abalone is presented in Fig. 15. The T_g' and T_m' are −44.3 and −18 °C, respectively.

Figure 16 presents the approximate ranges of T_m', T_g', X_s'' and T_{gs} of starch, protein and sugar-based systems in a state diagram based on the data in Tables 1, 2, 3, 4 and 5. The T_g' and T_m' of many food constituents ranged

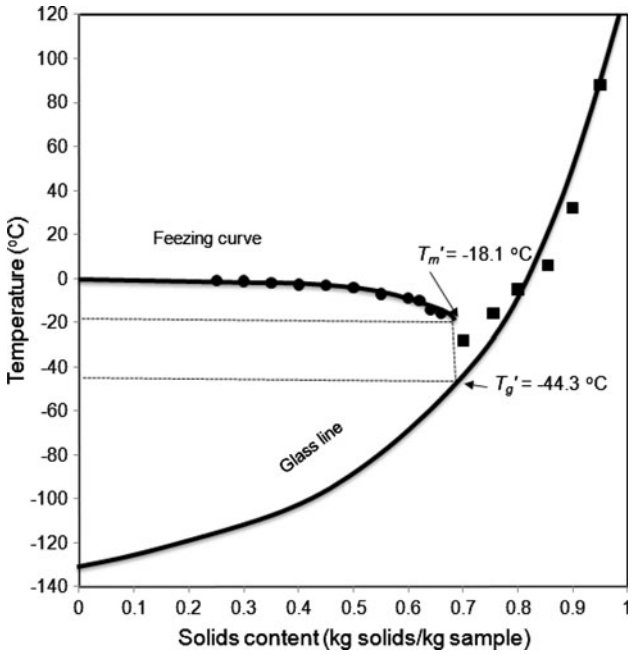

Fig. 15 State diagram of abalone proteins presenting glass line and melting curve; T_m', onset ice-melting temperature in a maximally freeze-concentrated solution; T_g' (Adapted from [177])

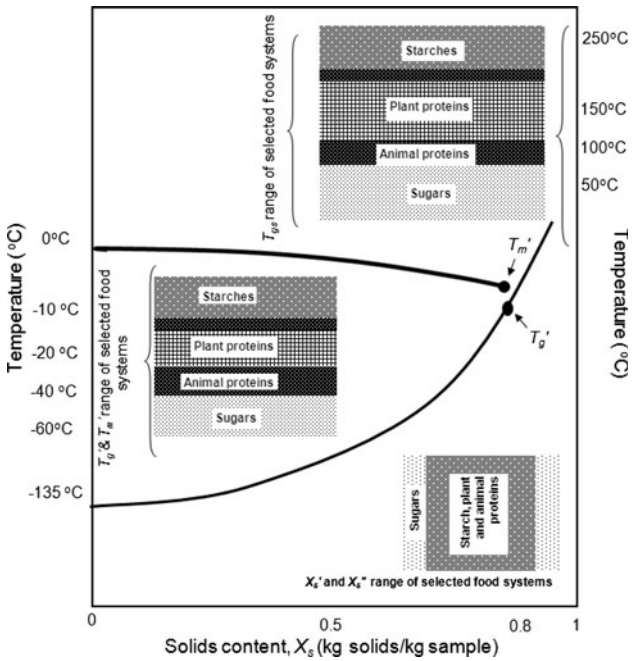

Fig. 16 State diagram presenting T_g', T_m', T_{gs}, X_s'' and X_s' range of food systems with selected major constituents. T_g', T_m', T_{gs} values of sugars and fruit solids are the lowest among the group, while food systems with large molecular weight components such as starches and proteins have greater T_g', T_m', T_{gs} values. X_s'' and X_s' values of sugars appear to have a broad range

from −5 to −70 °C, while the T_{gs} ranged from 30 to 300 °C. The unfrozen water of many food constituents varies between 20 and 30% (w.b.). Starches and proteins exhibit similar glass transition temperature ranges, while sugar systems exhibit a smaller range for glass transition temperatures.

Importance and Applications

State diagrams of food systems can be used to optimize processing and storage conditions by analyzing their glass lines, conditions of maximum-freeze-concentration and melting/freezing curves. Devitrification or glassy to rubbery transition is kinetic and promotes loss of quality and physiological activity in foods. Optimal processing conditions including temperature and relative humidity during selected food-processing operations (e.g., freeze-drying, extrusion, baking, frying, freeze concentration, storage and cryopreservation) can be predicted using state diagrams of the dominating food constituents. Sorption isotherms in combination with state diagrams may be useful for predicting adequate packaging requirements, optimal temperatures and relative humidities during storage.

Physical Stability

The major physical and structural deteriorative reactions that occur during processing and storage of foods are collapse of structure during freeze- and vacuum-drying [18, 93], stickiness of food powders during spray, hot air and fluidized bed drying and storage [4, 18], caking of food powders during storage [62], crystallization of sugar [38, 191] or loss of crispness [170]. Caking and crystallization are time-dependent and irreversible, while collapse and stickiness development are time-independent [18, 124].

The main reasons for collapse during or after dehydration and freeze-drying are low glass transition temperatures and high hygroscopicity, leading to undesirable quality attributes of foods [18, 107, 166, 176]. Most fruit solids exhibit a T_g' value between −10 and −60 °C, and their collapse temperature is also in this temperature range. Maintaining freeze-drying temperatures below the T_g' may avoid collapse and deterioration of the fruit structure. Sticking among food powder particles and the walls of containers often leads to poor product utility and productivity [18].

The combined effect of temperature and water affects the cohesion and stickiness of sugar-rich food powders [65]. For a storage temperature T, beyond a specific (T–T_g), amorphous components of food powders are sticky even after short time periods [137]. The magnitude of positive (T–T_g), rather than conditions resulting in differences between ambient and glass transition temperatures, is important for the development of stickiness in amorphous lactose during processing and storage. Temperature and water in amorphous components of food powders affect

plasticization and structural relaxation, resulting in sticky powders at a temperature called the sticky point temperature. Normally, the (T–T_g) is not greater than 10–20 °C, since the sticky point temperature of food powders occurs in this range [18].

Aguilera et al. [5] explained the stages of the caking phenomena in amorphous components of food powers. Positive values defining the differences between storage and glass transition temperatures (T–T_g) and relative humidity act as the driving forces that initiate caking over time. Fitzpatrick et al. [62] indicated that the cake strength of skim milk powder increases considerably when the (T–T_g) is greater than 20 °C. Along with glass transition temperature, many other factors such as time, storage temperature, water content and composition affect the caking behavior and cake strength of food powders.

Crystallization of sugars in carbohydrate-rich food systems is another concern of food technologists, since this adversely affects the physical quality, consumer acceptability and acceptable shelf life of many foods. Amorphous components of food powders may crystallize over time to approach greater stability. The crystallized state is organized with regular lattice structures, unlike the randomly arranged amorphous glassy structures. During crystal formation, adsorbed water in amorphous powders is released, resulting in plasticization of the amorphous material. The release of adsorbed water increases the water activity of foods, resulting in potential physicochemical deterioration in foods. Crystallization is a kinetic phenomena, and the temperature at which crystallization occurs is between the glass transition temperature and melting temperature of the amorphous components [115]. Suitable conditions to attain the crystallized state include high relative humidity (RH) and ambient temperature. As the difference between storage temperature and glass transition temperature increases, the rate of release of adsorbed water from food increases and crystallization occurs. Crystallization occurs at temperatures greater than and less than the glass transition temperature, but rates of crystallization are significantly different [223]. Crystallization may be delayed by storing foods and pharmaceuticals at safe storage temperatures referred as zero mobility temperature (T_o) [79, 223]. It is assumed that at T_o, no molecular relaxations are observed. T_o also corresponds to the theoretical Kauzman temperature of approximately 50 K below T_g. The value of T_o can be approximated with the Vogel–Tammann–Fulcher equation [79]. Along with this, storage time, food composition and molecular weight can also affect food crystallization [38]. The rate of crystallization is slow for high molecular weight components. Crystallization of amorphous components of food powders results in reduced solubility over time. A number of studies report crystallization of amorphous lactose and components of skim milk powder at temperatures greater than their glass transition temperatures [85, 87]. Lactose crystallization was observed in milk powders stored at temperatures greater than their glass transition temperatures or at critical water activities corresponding to their glass transition temperatures [85]. Like caking and stickiness, rate of crystallization also increases as water content or the difference between storage and glass transition temperature increases [157]. Crystallization and wall deposition of spray-dried food polymers may be reduced by producing spray-dried food polymers at a temperature less than the glass transition temperature [38].

Crispness is another sensory attribute that affects consumer acceptability. Loss of crispness in carbohydrate-rich foods during storage is related to depressed glass transition temperatures less than storage temperatures [170]. High molecular weight additives such as maltodextrins and gum arabic are encapsulating ingredients mixed with fruit juices for the retention of volatile ingredients. These additives increase glass transition temperatures during dehydration and storage [154]. The retention of volatiles in spray-dried microcapsules using mesquite gum reached the maximum when the microencapsulates were stored at temperatures lower than their T_g [17]. Spray-drying removes water and transforms food powders to the glassy state, improving flavor retention and reducing caking due to rapid drying and evaporative cooling [224].

By controlling the processing and storage temperature (T) of foods well below the glass transition temperatures and by adding high molecular weight ingredients with high T_g, adverse structural changes can be prevented to ensure acceptable food quality [94]. The temperature regions where stickiness, collapse and crystallization occur can be represented in a state diagram [124]. Maximum utilization of state diagrams is made by choosing optimum temperature and water concentrations to avoid detrimental effects of structural changes. Sorption isotherms and state diagrams along with (T–T_g) may be used to predict the physical stability of foods during processing, transport, packaging and storage [62].

Chemical Stability

Molecular motions are reduced considerably, and the rates of chemical reactions are also reduced in the glassy state of food polymers [190]. Several chemical and biochemical reactions in foods such as sucrose hydrolysis [30, 185], enzyme inactivation [36, 37, 184], non-enzymatic browning [13, 95], vitamin degradation [12, 179], protein denaturation [14, 47] and oxidation [55, 109, 190] are investigated in relation to glass transition temperatures and water mobility. The rates of many chemical reactions are influenced by water concentrations in foods. For example, rates of thiamin

and vitamin *C* degradation, lipid oxidation and the Maillard reaction increase as water concentrations increase and can be predicted by the glass transition temperatures and physical states of foods [10, 12, 55, 179]. However, several studies indicate that selected chemical reactions occur in the glassy state, suggesting that T_g alone cannot be considered an absolute threshold temperature for the chemical stability of foods. The influence of glass transition temperature on selected chemical reactions is not clear, because water exhibits multiple functions in foods as a plasticizer, solvent, reactant or product of chemical reactions [30]. The analysis of the impact of T_g on water mobility and chemical stability of polyvinylpyrrolidone (PVP) by nuclear magnetic resonance indicates that water mobility is not influenced by T_g [11]. Water mobility was observed in the glassy state of the PVP model system. Moreover, Bell et al. [11] reported that water mobility in the food system cannot be used as an indicator to explain the chemical stability of foods. Glass transition temperatures and the physical state of a system are not the only way to clarify complex chemical degradation reactions in food systems. Other factors, such as food constituents and constituent concentrations, play a major role in predicting and explaining deterioration resulting from chemical reactions.

Microbial Stability

Water activity is considered the single most valuable parameter in defining the microbial stability of intermediate and low-moisture foods. Foods with low water activities are normally in the amorphous glassy state, and the glassy state or low water activity may contribute to microbial stability. Slade and Levine [197] suggested that the glass transition concept or water dynamics may provide an alternative to water activity for the prediction of the microbial stability of low-moisture and intermediate-moisture foods. Chirife and Buera [39] concluded that the glass transition concept is not useful in predicting microbial growth in foods. They explained that water activity is a solvent property, whereas the glassy state is a solute and structure-related property, and both water activity and physical state in foods are required for understanding food–water relationships. Buera et al. [29] reported the presence of xerophilic molds in white bread in the glassy state stored at adequate water activities. They suggested that glassy and rubbery states may exist in food matrices with incompatible constituents. Chirife and Buera [39] indicated that molds may grow in substrates of relatively high T_g due to the presence non-glassy microregions. Champion et al. [33] also indicated that macroscopic heterogeneities in food materials can induce areas with greater water mobility. It is unlikely that the glass transition concept defining biopolymer mobility will be an adequate predictor of water activity, water mobility, microbial growth and survival, or food safety. Additional studies are needed to probe the utility of the glass transition concept to explain microbial stability.

Frozen Food Stability

Temperatures below T_g'' are desirable for safe storage of high water content food systems, since they consist of ice, glass and solute ([33]; 159). The T_g' of most foods ranges from −10 to −70 °C. It may not be economically feasible or practical to store sugar-rich foods such as fruits at temperatures below their T_g' (−40 to −70 °C). Maximum ice formation in the food systems during freezing takes place when systems are stored between their T_m' and T_g'. At temperatures greater than T_m', the food system may be plasticized by the melting of ice. This condition may result in a partial-freeze-concentration in the matrix and may not be suitable for long-term storage of foods. Both T_m' and T_g' are independent of initial food solids concentration [73]. The unfrozen water plasticizes the freeze-concentrated food matrix, so the quantity of unfrozen water provides valuable information for stable frozen storage of foods [162]. Unfrozen water is available to the solutes in the food system, unlike bound water, which is structurally and chemically bound to the solutes and unavailable for reactions. Ice recrystallization in foods may be reduced and food quality may be improved by storing the foods below their glass transition temperature [141]. T_m' and T_g' are important in cryostabilization and cryoprotection of foods at varied process and storage conditions. Reaction rates may be a function of $(T–T_g')$ and may increase with an increase in $(T–T_g')$, where T is the storage temperature.

Ferrero and Zaritzky [59] studied the amylopectin retrogradation and textural changes in frozen starch–sucrose–water systems after slow freezing and frozen storage. Amylopectin retrogradation was observed at storage temperature greater than T_g'. The addition of hydrocolloids such as gums did not inhibit the amylopectin retrogradation. Akkose and Aktas [6] reported that the total volatile basic nitrogen (TVB-N) and the thiobarbituric acid-reactive substances (TBARS) in ground beef differed significantly when stored above the T_g' for 6 months. However, storage studies of anthocyanins and soluble phenols in berry juices during frozen storage (between −10 and −30 °C) for 6 months showed that the stability of anthocyanins and soluble phenols are influenced by storage temperature and storage time [155]. The glass transition temperature of maximum-freeze-concentrated phases exhibited no influence on the stability of anthocyanins and soluble phenols. Torreggiani et al. [209] reported that no simple relationship was observed between anthocyanin loss in strawberry juices and the difference in the storage and glass transition

temperature of maximally freeze-concentrated phase (T_g'). Other factors such as freeze concentration level and pH may play a role in the anthocyanin stability in strawberry juice [209]. Terefe and Hendrickx [207] reported that the kinetics of pectin methylestarase-catalyzed de-esterification of pectin was less influenced by T_g'. Therefore, glass transition temperature may not be the single parameter controlling the frozen storage stability of foods, and more critical studies on stability of foods during frozen storage are needed.

Other Applications

Kaletunc and Breslauer [88] demonstrated the use of state diagrams in characterizing the physical states of wheat flour in selected unit operations prior to or during extrusion processing. They explained the influence of post-extrusion storage conditions on the state of extrudate by using a state diagram. State diagrams identify the temperature and water content at which the protein components of extruded or baked products become crispy by changing the glassy state [104]. Adulteration of honey, milk and fruit juices may be identified using the glass transition temperature concept analyzed by DSC [43, 76]. Including sorption isotherms in a single, modified state diagram can help researchers analyze, design and optimize process conditions, and select the packaging and storage environments [142]. The glass transition concept is applied to select the appropriate processing conditions such as drying temperature, relative humidity for maximum head rice yield and milling quality. The head rice yield decreases when drying is conducted in the rubbery state without tempering [41, 221, 222].

Summary and Future Research

State diagrams describing the physical states and state transitions of foods can function as significant tools to help food scientists, food engineers and food-packaging researchers develop processing protocols and determine storage conditions. Various thermal analytical and spectroscopic techniques are available for modeling and characterizing food components and relating observed transitions to food stability. This article described methods for determining and understanding state transitions of food component mixtures. Calorimetric determinations are the most common methods for characterization of phase/state transitions in food systems. Mechanical determinations combined with the free volume theory provide mechanistic understanding of rubber to glass transition in biomaterials. Spectroscopic methods such as NMR and EPR are used less often, yet they help researchers directly probe molecular mobility. Glass transition temperatures are often perceived as dependent on the method of observation and not well defined. There are some discrepancies in T_g determined using selected analytical techniques, since each technique probes material properties at atomic, micro- and macroscales to identify glass transition temperatures. More research is needed to develop standard experimental protocols for characterization of accurate glass transition temperatures with each determination technique.

We presented state diagrams for many pure food ingredients. State diagrams including glass transition and freezing curve data are mainly limited to fruits. Significant variations in glass transition temperatures obtained for the same food constituents are attributed to differences in determination techniques. Therefore, it is difficult to generalize and use the state diagrams for the design of processes and storage conditions. We also presented glass transition temperature data for proteins and carbohydrates, but little information is available related to melting and the condition of maximum-freeze-concentration (T_m' and T_g'). Large molecular weight solutes increase the glass transition temperature (T_g), initial melting point, T_g' and T_m' of foods. The glass transition temperature concept is used to predict physical changes including crystallization, caking, stickiness and collapse; however, the relationship of glass transition temperature to chemical reactions is not clear. A better fundamental understanding of the kinetic state of food biopolymers and information on the factors affecting the chemical reactions in foods is needed. A limited number of studies report chemical stability in high-moisture foods stored below T_m' and T_g'. The molecular mobility in foods below the glass transition temperature is characterized by using an enthalpy or mechanical relaxation method. This may elucidate rates of biopolymer reactions in the glassy state. Due to limited information on the relaxation kinetics of food materials, the relationship of relaxation kinetics to food stability is still largely unexplored. The use of state diagrams that include glass transition temperatures, melting curve data and relaxation kinetics data can help improve the processing and storage of food materials.

Acknowledgments This activity was funded, in part, with an Emerging Research Issues Internal Competitive Grant from the Agricultural Research Center and with a Biological and Organic Agriculture (BioAg) Program Grant from the Center for Sustaining Agriculture and Natural Resources at Washington State University.

References

1. Abiad MG, Carvajal MT, Campanella OH (2009) A review on methods and theories to describe the glass transition phenomenon: applications in food and pharmaceutical products. Food Eng Rev 1(2):105–132

2. Ablett S (1992) Overview of NMR applications in food science. Trends Food Sci Technol 31:246–250
3. Ablett S, Izzard MJ, Lillford PJ, Arvannitoyannis I, Blanshard JMV (1993) Calorimetric study of the glass transition occurring in fructose solutions. Carbohydr Res 246:13–22
4. Adhikari B, Howes T, Lecomte D, Bhandari BR (2005) A glass transition temperature approach for the prediction of the surface stickiness of a drying droplet during spray drying. Powder Technol 149:168–179
5. Aguilera JM, del Valle JM, Karel M (1995) Caking phenomena in amorphous food powders. Trends Food Sci Technol 6:149–155
6. Akkose A, Aktas N (2008) Determination of glass transition temperature of beef and effects of various cryoprotective agents on some chemical changes. Meat Sci 80:875–878
7. Allen SG (1993) A history of the glassy state. In: Blanshard JMV, Lillford PJ (eds) The glassy state in foods. Nottingham University Press, Loughborough
8. Arvanitoyannis I, Blanshard JMV, Ablett S, Izzard MJ, Lillford PJ (1993) Calorimetric study of the glass-transition occurring in aqueous glucose—fructose solutions. J Sci Food Agric 63: 177–188
9. Bai Y, Rahman MS, Perera CO, Smith B, Melton LD (2001) State diagram of apple slices: glass transition and freezing curves. Food Res Int 34:89–95
10. Bell LN, Touma DE, White KL, Chen Y (1998) Glycine loss and Maillard browning as related to the glass transition in a model food system. J Food Sci 63(4):625–628
11. Bell LN, Bell HM, Glass TE (2002) Water mobility in glassy and rubbery solids as determined by oxygen-17 nuclear-magnetic resonance: impact on chemical stability. Lebensm-wiss Technol 35(2):108–113
12. Bell LN, White KL (2000) Thiamin stability in solids as affected by the glass transition. J Food Sci 65(3):498–501
13. Bell LN (1995) Kinetics of non-enzymatic browning in amorphous solid systems: distinguishing the effects of water activity and the glass transition. Food Res Int 28(6):591–597
14. Bell LN, Hageman MJ (1996) Glass transition explanation for the effect of polyhydroxy compounds on protein denaturation in dehydrated solids. J Food Sci 61(2):372–374
15. Bell LN (2007) Moisture effects on food's chemical stability. In: Barbosa-Canovas GV, Fontana AJ Jr, Schmidt SJ, Labuza TP (eds) Water activity in foods: fundamentals and applications. Blackwell Publishing Ltd, Ames
16. Bengoechea C, Arrachid A, Guerrero A, Hill SE, Mitchell JR (2007) Relationship between the glass transition temperature and the melt flow behavior for gluten, casein and soya. J Cereal Sci 45:275–284
17. Beristain CI, Azuara E, Tamayo T, Vernon-Carter EJ (2003) Effect of caking and stickiness on the retention of spray-dried encapsulated orange peel oil. J Sci Food Agric 83(15):1613–1616
18. Bhandari BR, Howes T (1999) Implication of glass transition for the drying and stability of dried foods. J Food Eng 40:71–79
19. Bhandari BR, Howes T (2000) Glass transition in processing and stability of food. Food Aust 52(12):579–585
20. Bidstrup SA, Day DR (1994) Assignment of glass transition temperature using dielectric analysis: a review. In: Seyler RJ (ed) Assignment of the glass transition. ASTM, Philadelphia
21. Biliaderis CG, Swan RS, Arvannitoyannis I (1999) Physicochemical properties of commercial starch hydrolyzates in the frozen state. Food Chem 64(4):537–546
22. Bindzus W, Livings SJ, Gloria-Hernandez HG, Fayard G, Van Lengerich B, Meuser F (2002) Glass transition of extruded wheat, corn and rice starch. Starch 54:393–400
23. Blanshard JMV (1995) The glass transition, its nature, and significance in food processing. In: Becket ST (ed) Physicochemical aspects of food processing, Blackie Academic & Professional, Glasgow
24. Blond G, Simatos D, Catte M, Dussap CG, Gros JB (1997) Modeling of the water-sucrose state diagram below 0 degrees C. Carbohydr Res 298:139–145
25. Boonyai P, Bhandari B, Howes T (2006) Applications of thermal mechanical compression tests in food powder analysis. Int J Food Prop 9:127–134
26. Boonyai P, Howes T, Bhandari B (2007) Instrumentation and testing of a thermal mechanical compression test for glass-rubber transition analysis of food powders. J Food Eng 78:1333–1342
27. Brake NC, Fennema OR (1999) Glass transition values of muscle tissue. J Food Sci 64(1):10–15
28. Brent JL, Mulvaney SJ, Cohen C, Bartsch JA (1997) Thermomechanical glass transition of extruded cereal melts. J Cereal Sci 26:301–312
29. Buera MP, Jouppila K, Roos YH, Chirife J (1998) Differential scanning calorimetry glass transition temperatures of white bread and mold growth in the putative glassy state. Cereal Chem 75(1):64–69
30. Buera MP, Chirife J, Karel M (1995) A study of acid-catalyzed sucrose hydrolysis in an amorphous polymeric matrix at reduced moisture contents. Food Res Int 28(4):359–365
31. Buitink J, Hemminga MA, Hoekstra FA (1999) Characterization of molecular mobility in seed tissues: an electron paramagnetic resonance spin probe study. Biophys J 76:3315–3322
32. Buitink J, van den Dries IJ, Hoekstra FA, Alberda M, Hemminga MA (2000) High critical temperature above T-g may contribute to the stability of biological systems. Biophys J 79:1119–1128
33. Champion D, Le Meste M, Simatos D (2000) Towards an improved understanding of glass transition and relaxations in foods: molecular mobility in the glass transition range. Trends Food Sci Technol 11:41–55
34. Chartoff RP, Weissman PT, Sircar A (1994) The application of dynamic mechanical methods to T_g determination in polymers: an overview. In: Seyler RJ (ed) Assignment of the glass transition. ASTM, Philadelphia
35. Chen CS (1986) Effective molecular-weight of aqueous-solutions and liquid foods calculated from the freezing-point depression. J Food Sci 51:1537–1539
36. Chen YH, Aull JL, Bell LN (1999) Solid-state tyrosinase stability as affected by water activity and glass transition. Food Res Int 32(7):467–472
37. Chen YH, Aull JL, Bell LN (1999) Invertase storage stability and sucrose hydrolysis in solids as affected by water activity and glass transition. J Agric Food Chem 47(2):504–509
38. Chiou D, Langrish TAG (2007) Crystallization of amorphous components in spray-dried powders. Dry Technol 25(9):1427–1435
39. Chirife J, Buera MP (1994) Water activity, glass-transition and microbial stability in concentrated/semimoist food systems. J Food Sci 59(5):921–927
40. Chung H, Woo K, Lim S (2004) Glass transition and enthalpy relaxation of cross-linked corn starches. Carbohydr Polym 55:9–15
41. Cnossen AG, Siebenmorgen TJ, Yang W (2002) The glass transition temperature concept in rice drying and tempering: effect on drying rate. Trans ASAE 45(3):759–766
42. Coleman NJ, Craig DQM (1996) Modulated temperature differential scanning calorimetry: a novel approach to pharmaceutical thermal analysis. Int J Pharm 135:13–29
43. Cordella C, Antinelli JF, Aurieres C, Faucon JP, Cabrol-Bass D, Sbirrazzuoli N (2002) Use of differential scanning calorimetry (DSC) as a new technique for detection of adulteration in

honeys. 1. Study of adulteration effect on honey thermal behavior. J Agric Food Chem 50:203–208
44. Couchman PR, Karasz FF (1978) A classical thermodynamic discussion of the effect of composition on glass-transition temperatures. Macromolecules 11:117–119
45. Cuq B, Gontard N, Guilbert S (1997) Thermal properties of fish myofibrillar protein-based films as affected by moisture content. Polymer 38(10):2399–2405
46. Cuq B, Lcard-Verniere C (2001) Characterization of glass transition of durum wheat semolina using modulated differential scanning calorimetry. J Cereal Sci 33:213–221
47. D'Cruz NM, Bell LN (2005) Thermal unfolding of gelatin in solids as affected by the glass transition. J Food Sci 70(2):E64–E68
48. de Graaf EM, Madeka H, Cocero AM, Kokini JL (1993) Determination of the effect of moisture on gliadin glass-transition using mechanical spectrometry and differential scanning calorimetry. Biotechnol Prog 9:210–213
49. De Graaf RA, Karman AP, Janssen LPBM (2003) Material properties and glass transition temperatures of different thermoplastic starches after extrusion processing. Starch 55:80–86
50. Delgado AE, Sun D (2002) Desorption isotherms and glass transition temperature for chicken meat. J Food Eng 55:1–8
51. del Valle JM, Cudros TRM, Aguilera JM (1998) Glass transitions and shrinkage during drying and storage of osmosed apple pieces. Food Res Int 31(3):191–204
52. Diab T, Biliaderis CG, Gerasopoulos D, Sfakiotakis E (2001) Physicochemical properties and application of pullulan edible films and coatings in fruit preservation. J Sci Food Agric 81: 988–1000
53. Di Gioia L, Cuq B, Guilbert S (1999) Thermal properties of corn gluten meal and its proteic components. Int J Biol Macromol 24:341–350
54. Dlubek G, Fretwell HM, Alam MA (2000) Positron/positronium annihilation as a probe for the chemical environment of free volume holes in polymers. Macromolecules 33(1):187–192
55. Drusch S, Serfert Y, Van Den Heuvel A, Schwarz K (2006) Physicochemical characterization and oxidative stability of fish oil encapsulated in an amorphous matrix containing trehalose. Food Res Int 39(7):807–815
56. Earnest CM (1994) Assignment of the glass transition temperatures using thermomechanical analysis. In: Seyler RJ (ed) Assignment of the glass transition. ASTM, Philadelphia
57. Farhat IA (2004) Measuring and modeling the glass transition temperature. In: Steele R (ed) Understanding and measuring the shelf-life of food. CRC Press, New York
58. Farkas J, Mohacsi-Farkas C (1996) Application of differential scanning calorimetry in food research and food quality assurance. J Therm Anal 47:1787–1803
59. Ferrero C, Zaritzky N (2000) Effect of freezing rate and frozen storage on starch-sucrose-hydrocolloid systems. J Sci Food Agric 80:2149
60. Ferry JD (1980) Viscoelastic properties of polymers. Wiley, NewYork
61. Fessas D, Schiraldi A (2001) State diagrams of arabinoxylan-water binaries. Thermochim Acta 370(1–2):83–89
62. Fitzpatrick JJ, Hodnett M, Twomey M, Cerqueira PSM, O'Flynn J, Roos YH (2007) Glass transition and the flowability and caking of powders containing amorphous lactose. Powder Technol 178:119–128
63. Fonseca F, Obert JP, Beal C, Marin M (2001) State diagrams and sorption isotherms of bacterial suspensions and fermented medium. Thermochim Acta 366:167–182
64. Forssel PM, Mikkila JM, Moates GK, Parker R (1997) Phase and glass transition behavior of concentrated barley starch-glycerol-water mixtures, a model for thermoplastic starch. Carbohdr Polym 34:275–282
65. Foster KD, Bronlund JE, Paterson AHJ (2006) Glass transition related cohesion of amorphous sugar powders. J Food Eng 77:997–1006
66. Fox TG, Flory PJ (1950) Second order transition temperatures and related properties of polystyrene .1. Influence of molecular weight. J Appl Phys 21:581–591
67. Franks F (1986) Metastable water at subzero temperatures. J Microsc 141(3):243–249
68. Franks F (1986) Unfrozen water—yes—unfreezable water—hardly—bound water—certainly not. Cryoletters 7(4):207–211
69. Franks F (1991) Water activity: a credible measure of food safety and quality? Trends Food Sci Technol 2:68–72
70. Gedde UW (1995) Polymer physics. Chapman and Hall, London
71. Gibbs JH, DiMarzio EA (1958) Nature of the glass transition and the glassy state. J Chem Phys 28:373–383
72. Goff HD, Caldwell KB, Stanley DW, Maurice TP (1993) The influence of polysaccharides on the glass-transition in frozen sucrose solutions and ice-cream. J Dairy Sci 76:1268–1277
73. Goff HD, Sahagian ME (1996) Glass transitions in aqueous carbohydrate solutions and their relevance to frozen food stability. Thermochim Acta 280/281:449–464
74. Goff HD (1995) The use of thermal-analysis in the development of a better understanding of frozen food stability. Pure Appl Chem 67(11):1801–1808
75. Gordon M, Taylor JS (1952) Ideal copolymers and the second order transitions of synthetic rubbers. I. Noncrystalline copolymers. J Appl Chem 2:493–500
76. Goswami TK, Gupta SK (2008) Detection of dilution of milk with the help of glass transition temperature by differential scanning calorimetry (DSC). Afr J Food Sci 2:7–10
77. Goula AM, Karapantsios TD, Achilias DS, Adamopoulos KG (2008) Water sorption isotherms and glass transition temperature of spray dried tomato pulp. J Food Eng 85(1):73–83
78. Gray R (1995) Electron spin resonance spectroscopy for detection of irradiated foods. In: Dickinson E (ed) New physicochemical techniques for the characterization of complex food systems. Chapman and Hall, London
79. Hancock BC, Zografi G (1997) Characteristics and significance of the amorphous state in pharmaceutical systems. J Pharm Sci 86(1):1–12
80. Hansen E, Lauridsen L, Skibsted LH, Moawad RK, Anderson ML (2004) Oxidative stability of frozen pork patties: effect of fluctuating temperature on lipid oxidation. Meat Sci 68: 185–191
81. Hashimoto T, Suzuki T, Hagiwara T, Takai R (2004) Study on the glass transition for several processed fish muscles and its protein fractions using differential scanning calorimetry. Fish Sci 70:1144–1152
82. Hutchinson JM (1995) Physical aging of polymers. Prog Pol Sci 20(4):703–760
83. Israkarn K, Charoenrein S (2006) Influence of annealing temperature on Tg′ of cooked rice stick noodles. Int J Food Prop 9:759–766
84. Johari GP, Hallbrucker A, Mayer E (1987) The glass liquid transition of hyperquenched water. Nature 330:552–553
85. Jouppila K, Roos YH (1994) Glass transitions and crystallization in milk powders. J Dairy Sci 77:2907–2915
86. Jouppila K, Roos YH (1997) The physical state of amorphous corn starch and its impact on crystallization. Carbohydr Polym 32:95–104
87. Jouppila K, Kansikas J, Roos YH (1997) Glass transition, water plasticization, and lactose crystallization in skim milk powder. J Dairy Sci 80:3152–3160

88. Kaletunc G, Breslauer KJ (1996) Construction of a wheat–flour state diagram: application to extrusion processing. J Therm Anal 47(5):1267–1288
89. Kaletunc G, Breslauer KJ (2003) Calorimetry of pre and postextruded cereal flours. In: Kaletunc G, Breslauer KJ (eds) Characterization of cereals and flours. Marcel Dekker Inc, New York
90. Kalichevsky MT, Jaroszkiewicz JM, Ablett S, Blanshard JMV, Lillford PJ (1992) The glass transition of amylopectin measured by dsc, dmta and nmr. Carbohydr Polym 18(2):77–88
91. Kalichevsky MT, Blanshard JMV, Tokarczuk PF (1993) Effect of water content and sugars on the glass-transition of casein and sodium caseinate. Int J Food Sci Technol 28(2):139–151
92. Kantor Z, Pitsi G, Thoen J (1999) Glass transition temperature of honey as a function of water content as determined by differential scanning calorimetry. J Agric Food Chem 47(6):2327–2330
93. Karathanos V, Angelea S, Karel M (1993) Collapse of structure during drying of celery. Dry Technol 11:1005–1023
94. Karel M, Anglea S, Buera P, Karmas R, Levi G, Roos YH (1994) Stability related transitions of amorphous foods. Thermochim Acta 246:249–269
95. Karmas R, Buera MP, Karel M (1992) Effect of glass-transition on rates of nonenzymatic browning in food systems. J Agric Food Chem 40(5):873–879
96. Kasapis S, Rahman MS, Guizani N, Al-Aamri M (2000) State diagram of temperature vs date solids obtained from the mature fruit. J Agric Food Chem 48:3779–3784
97. Kasapis S, Sablani SS (2005) A fundamental approach for the estimation of the mechanical glass transition temperature in gelatin. Int J Biol Macromol 36:71–78
98. Kasapis S (2004) Definition of a mechanical glass transition temperature for dehydrated foods. J Agric Food Chem 52(8): 2262–2268
99. Kasapis S (2008) Recent advances and future challenges in the explanation and exploitation of the network glass transition of high sugar/biopolymer mixtures. Crit Rev Food Sci Nutr 48(2): 185–203
100. Katayama DS, Carpenter JF, Manning MC, Randolph TW, Setlow P, Menard KP (2008) Characterization of amorphous solids with weak glass transitions using high ramp rate differential scanning calorimetry. J Pharm Sci 97(2):1013–1024
101. Katekawa EK, Silva MA (2007) On the influence of glass transition on shrinkage in convective drying of fruits: a case study of banana drying. Dry Technol 25:1659–1666
102. Kelley FN, Bueche F (1961) Viscosity and glass–temperature relations for polymer-diluent systems. J Pol Sci 50:549–556
103. Khalloufi S, El-Maslouhi Y, Ratti C (2000) Mathematical model for prediction of glass transition temperature of fruit powders. J Food Sci 65(5):842–848
104. Kokini JL, Cocero AM, Madeka H, de Graaf E (1994) The development of state diagrams for cereal proteins. Trends Food Sci Technol 5:281–288
105. Kokini JL, Cocero AM, Madeka H (1995) State diagrams help predict rheology of cereal proteins. Food Technol 49(10):74–82
106. Kou Y, Molitor PF, Schmidt SJ (1999) Mobility and stability characterization of model food systems using NMR, DSC, and conidia germination techniques. J Food Sci 64(6):950–959
107. Krokida MK, Karathanos VT, Maroulis ZB (1998) Effect of freeze-drying conditions on shrinkage and porosity of dehydrated agricultural products. J Food Eng 35:369–380
108. Kwei TK (1984) The effect of hydrogen bonding on the glass transition temperatures of polymer mixtures. J Polym Sci Lett Edit 22:307–313
109. Labrousse S, Roos YH, Karel M (1992) Collapse and crystallization in amorphous matrices with encapsulated compounds. Sci Aliments 12(4):757–769
110. Laaksonen TJ, Roos YH (2000) Thermal, dynamic-mechanical, and dielectric analysis of phase and state transitions of frozen wheat doughs. J Cereal Sci 32(3):281–292
111. Laaksonen TJ, Roos YH (2003) Water sorption and dielectric relaxations of wheat dough (containing sucrose, NaCl, and their mixtures). J Cereal Sci 37:319–326
112. Lai VMF, Lii CY (1999) Effects of modulated differential scanning calorimetry (MDSC) variables on thermodynamic and kinetic characteristics during gelatinization of waxy rice starch. Cereal Chem 76(4):519–525
113. Lazaridou A, Biliaderis CG (2002) Thermophysical properties of chitosan, chitosan-starch and chitosan-pullulan films near the glass transition. Carbohydr Polym 48:179–190
114. Lazaridou A, Biliaderis CG, Bacandritsos N, Sabatini AG (2004) Composition, thermal and rheological behavior of selected Greek honeys. J Food Eng 64:9–21
115. Le Meste M, Champion D, Roudaut G, Blond G, Simatos D (2002) Glass transition and food technology: a critical appraisal. J Food Sci 67(7):2444–2458
116. Le Meste M, Huang V (1992) Thermomechanical properties of frozen sucrose solutions. J Food Sci 57(5):1230–1233
117. Levine H, Slade L (1986) A polymer physicochemical approach to the study of commercial starch hydrolysis products. Carbohydr Polym 6:213–244
118. Li Y, Kloeppel KM, Hsieh F (1998) Texture of glassy corn cakes as a function of moisture content. J Food Sci 63(5):869–872
119. Li S, Dickinson LC, Chinachoti P (1998) Mobility of "unfreezable" and "freezable" water in waxy corn starch by H-2 and H-1 NMR. J Agric Food Chem 46:62–71
120. Lim M, Wu H, Breckel M, Birch J (2006) Influence of the glass transition and storage temperature of frozen peas on the loss of quality attributes. Int J Food Sci Technol 41:507–512
121. Lin AA, Kwei TK, Reiser A (1989) On the physical meaning of the Kwei equation for the glass-transition temperature of polymer blends. Macromolecules 22:4112–4119
122. Lin X, Ruan RR, Chen P, Chung M, Ye X, Yang T, Doona C, Wagner T (2006) NMR state diagram concept. J Food Sci 71(9): 136–144
123. Madeka H, Kokini JL (1996) Effect of glass transition and cross-linking on rheological properties of zein: development of a preliminary state diagram. Cereal Chem 73(4):433–438
124. Maltini E, Torreggiani D, Venir E, Bertolo G (2003) Water activity and the preservation of plant foods. Food Chem 82:79–86
125. Martinez-Navarrete N, Moraga G, Talens P, Chiralt A (2004) Water sorption and plasticization effect in wafers. Int J Food Sci Technol 39:555–562
126. Matveev YI, Grinberg VY, Tolstoguzov VB (2000) The plasticizing effect of water on proteins, polysaccharides and their mixtures. Glassy state of biopolymers, food and seeds. Food Hydrocoll 14:425–437
127. Matveev YI, Ablett S (2002) Calculation of the C′g and T′g intersection point in the state diagram of frozen solutions. Food Hydrocoll 16:419–422
128. Matveev YI (2004) Modification of the method for calculation of the C′(g) and T′(g) intersection point in state diagrams of frozen solutions. Food Hydrocoll 18:363–366
129. Micard V, Guilbert S (2000) Thermal behavior of native and hydrophobized wheat gluten, gliadin and glutenin-rich fractions by modulated DSC. Int J Biol Macromol 27:229–236
130. Modulated DSC™ Compendium. Theory and experimental conditions, TA applications brief, TA Instruments, New Castle
131. Morales A, Kokini JL (1999) State diagrams of soy globulins. J Rheol 43(2):315–325
132. Mousia Z, Farhat IA, Blachot JF, Mitchell JR (2000) Effect of water partitioning on the glass-transition behaviour of phase

separated amylopectin-gelatin mixtures. Polymer 41(5):1841–1848
133. Nelson KA, Labuza TP (1994) Water activity and food polymer science: implications of state on arrhenius and WLF models in predicting shelf-life. J Food Eng 22(1–4):271–289
134. Nikolaidis A, Labuza TP (1996) Glass transition state diagram of a baked cracker and its relationship to gluten. J Food Sci 61:803–806
135. Noel TR, Parker R, Ring SG, Tatham AS (1995) The glass-transition behavior of wheat gluten proteins. Int J Biol Macromol 17(2):81–85
136. Ohkuma C, Kawai K, Viriyarattanasak C, Mahawanich T, Tantratian S, Takai R, Suzuki T (2008) Glass transition properties of frozen and freeze-dried surimi products: effects of sugar and moisture on the glass transition temperature. Food Hydrocoll 22(2):255–262
137. Paterson AHJ, Brooks GF, Bronlund JE, Foster KD (2005) Development of stickiness in amorphous lactose at constant T-Tg levels. Int Dairy J 15(5):513–519
138. Peleg M (1996) On modeling changes in food and biosolids at and around their glass transition temperature range. Crit Rev Food Sci Nutr 38(1–2):49–67
139. Perdon A, Siebenmorgen TJ, Mauromoustakos A (2000) Glassy state transition and rice drying: development of a brown rice state diagram. Cereal Chem 77:708–713
140. Pouplin M, Redl A, Gontard N (1999) Glass transition of wheat gluten plasticized with water, glycerol, or sorbitol. J Agri Food Chem 47(2):538–543
141. Rahman MS (1995) Food properties handbook. CRC Press, Boca Raton
142. Rahman MS (2006) State diagram of foods: its potential use in food processing and product stability. Trends Food Sci Technol 17:129–141
143. Rahman MS (2004) State diagram of date flesh using differential scanning calorimetry (DSC). Int J Food Prop 7(3):407–428
144. Rahman MS, Sablani SS, Al-Habsi N, Al-Maskri S, Al-Belushi R (2005) State diagram of freeze-dried garlic powder by differential scanning calorimetry and cooling curve methods. J Food Sci 70(2):135–141
145. Rahman MS, Labuza TP (1999) Water activity and food preservation. In: Rahman MS (ed) Handbook of food preservation. Marcel Dekker, New York
146. Rahman MS, Kasapis S, Guizani N, Al-Amri OS (2003) State diagram of tuna meat: freezing curve and glass transition. J Food Eng 57:321–326
147. Rahman MS, Al-Marhubi IM, Al-Mahrouqi A (2007) Measurement of glass transition temperature by mechanical (DMTA), thermal (DSC and MDSC), water diffusion and density methods: a comparison study. Chem Phys Lett 440: 372–377
148. Rahman MS, Guizani N, Al-Khaseibi M, Al-Hinai SA, Al-Maskri SS, Al-Hamhami K (2002) Analysis of cooling curve to determine the end point of freezing. Food Hydrocoll 16:653–659
149. Rahman MS (2009) Food stability beyond water activity and glass transtion: macro-micro region concept in the state diagram. Int J Food Prop 12:726–740
150. Rahman MS, Machado-Velasco KM, Sosa-Morales ME, Velez-Ruiz JF (2009) Freezing point: measurement, prediction and data. In: Rahman MS (ed) Food properties handbook, 2nd edn. CRC Press, Taylor and Francis Group, New York
151. Rasanen J, Blanshard JMV, Mitchell JR, Derbyshire W, Autio K (1998) Properties of frozen wheat doughs at subzero temperatures. J Cereal Sci 28:1–14
152. Reid DS (1990) Optimizing the quality of frozen foods. Food Technol 44(7):78–84
153. Reid DS, Fennema O (2007) Water and ice. In: Damodaran S, Parkin KL, Fennema O (eds) Fennema's food chemistry, 4th edn. CRC Press, Taylor and Francis Group, New York
154. Righetto AM, Netto FM (2005) Effect of encapsulating materials on water sorption, glass transition and stability of juice from immature acerola. Int J Food Prop 8:337–346
155. Rizzolo A, Nani RC, Viscardi D, Bertolo G, Torreggiani D (2003) Modification of glass transition temperature through carbohydrates addition and anthocyanin and soluble phenol stability of frozen blueberry juices. J Food Eng 56:229–231
156. Rolee A, LeMeste M (1999) Effect of moisture content on thermomechanical behavior of concentrated wheat starch-water preparations. Cereal Chem 76(3):452–458
157. Roos YH, Karel M (1991) Applying state diagrams to food-processing and development. Food Technol 45(12):66–71
158. Roos YH, Karel M (1991) Water and molecular-weight effects on glass transitions in amorphous carbohydrates and carbohydrate solutions. J Food Sci 56(6):1676–1681
159. Roos YH, Karel M (1991) Amorphous state and delayed ice formation in sucrose solutions. Int J Food Sci Technol 26:553–566
160. Roos YH (1993) Water activity and physical state effects on amorphous food stability. J Food Process Preserv 16: 433–447
161. Roos YH (1993) Melting and glass transitions of low-molecular-weight carbohydrates. Carbohydr Res 238:29–48
162. Roos YH (1995) Glass transition-related physicochemical changes in foods. Food Technol 49(10):97–102
163. Roos YH (1995) Characterization of food polymers using state diagrams. J Food Eng 24:339–360
164. Roos YH (1995) Phase transitions in foods. Academic press, San Diego, CA
165. Roos YH, Karel M, Kokini JL (1996) Glass transitions in low-moisture and frozen foods: effects on shelf life and quality. Food Technol 50(11):95–108
166. Roos YH (1997) Frozen state transitions in relation to freeze drying. J Therm Anal 48(3):535–544
167. Roos YH (2003) Thermal analysis, state transitions and food quality. J Therm Anal Calorim 71(1):197–203
168. Roos YH (2007) Phase transitions and transformations in food systems. In: Heldman DR, Lund DB (eds) Handbook of food engineering. CRC Press, Boca Raton
169. Roos YH (2010) Glass transition temperature and its relevance in food processing. Annu Rev Food Sci Technol 1:469–496
170. Roudaut G, Dacremont C, Valles Pamies B, Colas B, Le Meste M (2002) Crispness: a critical review on sensory and material science approaches. Trends Food Sci Technol 13:217–227
171. Rouilly A, Orliac O, Silvestre S, Rigal L (2001) DSC study on the thermal properties of sunflower proteins according to their water content. Polymer 42:10111–10117
172. Ruan RR, Long Z, Song A, Chen PL (1998) Determination of the glass transition temperature of food polymers using low field NMR. Lebensm Wiss uTechnol 31:516–521
173. Ruan RR, Chen PL (1998) Water in foods and biological materials—a nuclear magnetic resonance approach. Technomic. Lancaster
174. Ruan RR, Long Z, Chang K, Chen PL, Taub IA (1999) Glass transition temperature mapping using magnetic resonance imaging. Trans ASAE 42(4):1055–1059
175. Sa MM, Sereno AM (1994) Glass transitions and state diagrams for typical natural fruits and vegetables. Thermochim Acta 246:285–297
176. Sablani SS, Rahman MS (2002) Pore formation in selected foods as a function of shelf temperature during freeze drying. Dry Technol 20(7):1379–1391

177. Sablani SS, Kasapis S, Rahman MS, Al-Jabri A, Al-Habsi N (2004) Sorption isotherms and the state diagram for evaluating stability criteria of abalone. Food Res Int 37:915–924
178. Sablani SS, Kasapis S (2006) Glass transition and water activity of freeze-dried shark. Dry Technol 24:1003–1009
179. Sablani SS, Al-Belushi K, Al-Marhubi I, Al-Belushi R (2007) Evaluating stability of vitamin C in fortified formula using water activity and glass transition. Int J Food Prop 10:61–71
180. Sablani SS, Kasapis S, Rahman MS (2007) Evaluating water activity and glass transition concepts for food stability. J Food Eng 78(1):266–271
181. Sablani SS, Rahman MS, Al-Busaidi S, Guizani N, Al-Habsi N, Al-Belushi R, Soussi B (2007) Thermal transitions of king fish whole muscle, fat and fat-free muscle by differential scanning calorimetry. Thermochim Acta 462:56–63
182. Sablani SS, Bruno L, Kasapis S, Syamaladevi RM (2009) Thermal transitions of rice: development of a state diagram. J Food Eng 90(1):110–118
183. Sacha GA, Nail SL (2009) Thermal analysis of frozen solutions: multiple glass transitions in amorphous systems. J Pharm Sci 98:3397–3405
184. Schebor C, Buera MD, Chirife J (1996) Glassy state in relation to the thermal inactivation of the enzyme invertase in amorphous dried matrices of trehalose, maltodextrin and PVP. J Food Eng 30(3–4):269–282
185. Schebor C, Buera MD, Chirife J, Karel M (1995) Sucrose hydrolysis in glassy starch matrix. Food Sci Technol 28(2): 245–248
186. Schmidt SJ (1999) Probing the physical and sensory properties of food systems using NMR spectroscopy. In: Belton PS, Hills BP, Webb GA (eds) Advances in magnetic resonance in food science. The Royal Society of Chemistry, UK
187. Schmidt SJ (2007) Water mobility in foods. In: Barbosa-Canovas GV, Fontana AJ, Schmidt SJ, Labuza TP (eds) Water activity in foods: principles and applications. Blackwell publishing, USA
188. Schmidt SJ (2004) Water and solids mobility in foods. In: Taylor S (ed) Advances in food and nutrition research. Academic Press, London
189. Sherwin CP, Labuza TP, McCormick A, Chen B (2002) Cross-polarization/magic angle spinning NMR to study glucose mobility in a model intermediate-moisture food system. J Agric Food Chem 50(26):7677–7683
190. Shimada Y, Roos YH, Karel M (1991) Oxidation of methyl linoleate encapsulated in amorphous lactose-based food model. J Agric Food Chem 39:637–641
191. Shrestha AK, Howes T, Adhikari BP, Bhandari BR (2008) Spray drying of skim milk mixed with milk permeate: effect on drying behavior, physicochemical properties, and storage stability of powder. Dry Technol 26:239–247
192. Silva MA, Sobral PJA, Kieckbusch TG (2006) State diagrams of freeze-dried camu-camu (Myrciaria dubia (HBK) Mc Vaugh) pulp with and without maltodextrin addition. J Food Eng 77: 426–432
193. Simatos D, Faure M, Bounjour E, Couch M (1975) The physical state of water at low thermal analysis and differential scanning calorimetry. Cryobiology 12:202–208
194. Simatos D, Blond G, Le Meste M (1989) Relation between glass-transition and stability of a frozen product. Cryo-Letters 10:77–84
195. Simatos D, Blond G, Roudaut G, Champion D, Perez J, Faivre AL (1996) Influence of heating and cooling rates on the glass transition temperature and the fragility parameter of sorbitol and fructose as measured by DSC. J Therm Anal 47:1419–1436
196. Singh KJ, Roos YH (2005) Frozen state transitions of sucrose-protein-cornstarch mixtures. J Food Sci 70(3):198–204
197. Slade L, Levine H (1987) Structural stability of intermediate moisture foods—a new understanding. In: Mitchell JR, Blanshard JMV (eds) Food structure—its creation and evaluation. Butterworths, London
198. Slade L, Levine H (1988) Non-equilibrium melting of native granular starch.1. Temperature location of the glass-transition associated with gelatinization of a-type cereal starches. Carbohydr Polym 8:183–208
199. Slade L, Levine H (1988) Non-equilibrium behavior of small carbohydrate-water systems. Pure Appl Chem 60:1841–1864
200. Slade L, Levine H (1991) Beyond water activity: recent advances based on an alternative approach to the assessment of food quality and safety. Crit Rev Food Sci Nutr 30:115–360
201. Syamaladevi RM, Sablani SS, Tang J, Powers J, Swanson BG (2009) State diagram and water adsorption isotherm of raspberry (*Rubus idaeus*). J Food Eng 91:460–467
202. Syamaladevi RM, Sablani SS, Tang J, Powers J, Swanson BG (2010) Water sorption and glass transition temperatures in red raspberry (*Rubus idaeus*). Thermochim Acta. doi: 10.1016/j.tca.2010.03.013
203. Tan I, Wee CC, Sopade PA, Halley PJ (2004) Investigation of the starch gelatinization phenomena in water-glycerol systems: application of modulated temperature differential scanning calorimetry. Carbohydr Polym 58:191–204
204. Telis VRN, Sobral PJA (2001) Glass transitions and state diagram for freeze-dried pineapple. Lebensm-wiss Technol 34:199–205
205. Telis VRN, Sobral PJA (2002) Glass transitions for freeze-dried and air-dried tomato. Food Res Int 35:435–443
206. Telis VRN, Sobral PJD, Telis-Romero J (2006) Sorption isotherm, glass transitions and state diagram for freeze-dried plum skin and pulp. Food Sci Technol Int 12(3):181–187
207. Terefe NS, Hendrickx M (2002) Kinetics of the pectin methylesterase catalyzed de-esterification of pectin in frozen food model systems. Biotechnol Prog 18(2):221–228
208. Tolstoguzov VB (2000) The importance of glassy biopolymer components in food. Nahr Food 44(2):76–84
209. Torreggiani D, Forni E, Guercilena I, Maestrelli A, Bertolo G, Archer GP, Kennedy CJ, Bone S, Blond G, Contreras-Lopez E, Champion D (1999) Modification of glass transition temperature through carbohydrates additions: effect upon color and anthocyanin pigment stability in frozen strawberry juices. Food Res Int 32:441–446
210. Toufeili I, Lambert IA, Kokini JL (2002) Effect of glass transition and cross-linking on rheological properties of gluten: development of a preliminary state diagram. Cereal Chem 79(1):138–142
211. Truong V, Bhandari BR, Howes T, Adhikari B (2002) Analytical model for the prediction of glass transition temperature of food systems. In: Levine H (ed) Amorphous food and pharmaceutical systems. The Royal society of chemistry, Cambridge
212. Van Nieuwenhuijzen NH, Primo-martin C, Meinders MBJ, Tromp RH, Hamer RJ, Van Vliet T (2008) Water content or water activity: what rules crispy behavior in bread crust? J Agric Food Chem 56:6432–6438
213. Vassilikou-Dova A, Kalogeras IM (2009) Dielectric analysis (DEA). In: Menczel JD, Prime RB (eds) Thermal analysis of polymers. Wiley, New Jersey
214. Vuataz G (2002) The phase diagram of milk: a new tool for optimizing the drying process. Lait 82:485–500
215. Wang H, Zhang S, Cuen G (2008) Glass transition and state diagram for fresh and freeze-dried Chinese gooseberry. J Food Eng 84:307–312
216. Ward IM, Hadley DW (1993) An introduction to the mechanical properties of solid polymers. Wiley, Chichester

217. Welti-Chanes J, Guerrero JA, Barcenas ME, Aguilera JM, Vergara F, Barbosa-Canovas GV (1999) Glass transition temperature (T_g) and water activity (a_w) of dehydrated apple products. J Food Process Eng 22(2):91–101
218. White GW, Cakebread SH (1966) The glassy state in certain sugar containing food products. J Food Technol 1:73–82
219. Wolfe J, Bryant G, Koster KL (2002) What is 'unfreezable water', how unfreezable is it and how much is there? CryoLetters 23:157–166
220. Wu X, Zhu Z (2009) Dynamic crossover of alpha relaxation in poly(vinyl acetate) above glass transition via mechanical spectroscopy. J Phys Chem B 113:11147–11152
221. Yang W, Jia C, Siebennorgen TJ, Pan Z, Cnossen AG (2003) Relationship of kernel moisture content gradients and glass transition temperatures to head rice yield. Biosyst Eng 85(4):467–476
222. Yang W, Jia C (2004) Glass transition mapping inside a rice kernel. Trans ASAE 47(6):2009–2015
223. Yu X, Kappes SM, Bello-Perez LA, Schmidt SJ (2008) Investigating the moisture sorption behavior of amorphous sucrose using a dynamic humidity generating instrument. J Food Sci 73(1):E25–E35
224. Zasypkin D, Porzio M (2004) Glass encapsulation of flavors with chemically modified starch blends. J Microencapsul 21(4): 385–397
225. Zhong Z, Sun XS (2005) J Food Eng 69:453–459